Solution Mining Research Institute, Spring 2006 Technical Meeting
Brussels, Belgium, May 1-3, 2006

IN SITU MECHANICAL TESTS IN SALT CAVERNS

Pierre Bérest[1], Mehdi Karimi-Jafari[1], Benoît Brouard[2], and Behrouz Bazargan[3]

[1] Laboratoire de Mécanique des Solides, Ecole Polytechnique, Palaiseau, France
[2] Brouard Consulting, Paris, France
[3] Bureau de Recherches Géologiques et Minières, Orléans, France

This paper was first published in the SMRI Technical Class Proceedings of the 2005 Spring Meeting in Syracuse, New York. SMRI Leadership and Kurt Staudtmeister, Coordinator of the Syracuse Technical Class, kindly authorized presentation of a slightly revised version of this paper for the SMRI Brussels Meeting.

1. INTRODUCTION

1.1. Mechanical Behavior of a Rock Sample

Many laboratory experiments have been devoted to the mechanical behavior of salt. Most authors agree on the following: The overall strain rate, $\dot{\varepsilon}$, of a sample submitted after time $t = 0$ to a constant load, σ, is the sum of elastic, steady-state and transient parts.

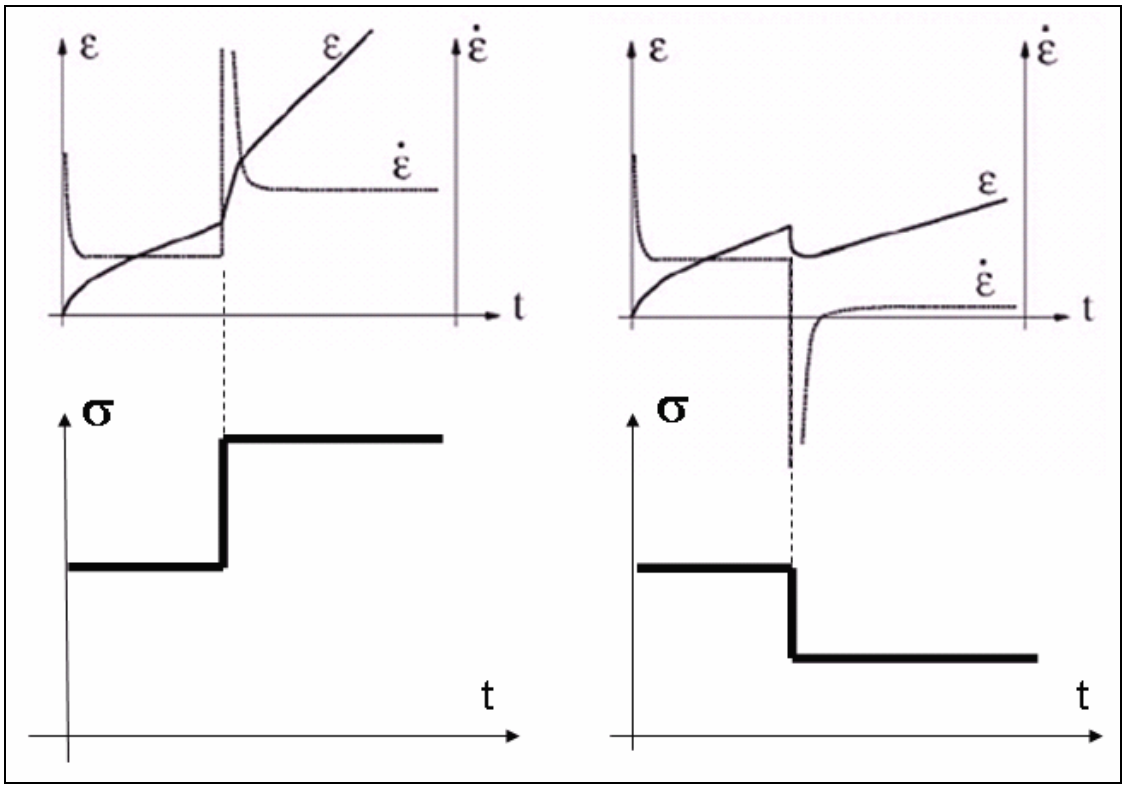

Figure 1 – Strain and strain rate as functions of time during a creep test: Cases of load increase (left) and load decrease (right) are considered. A stress drop (right) may trigger reverse creep. (Sample height increases for a while, even if the stress applied to the sample is compressive.)

The elastic part is small and is described by a linear relation between $\dot{\varepsilon}$ and $\dot{\sigma}$. The steady-state part is characterized by a constant strain rate reached after some days or weeks when a constant mechanical load is applied. The transient part describes rock behavior before steady state is reached. Any change in applied loading triggers transient creep. A stress drop may trigger transient "reverse" creep, or $\dot{\varepsilon} < 0$ (see Figure 1).

Rock failure is reached when:

(a) a sample is submitted to a (small) tensile stress; or

(b) a sample is submitted to a (relatively high) compressive state of stress. It generally is accepted that a short-term failure criterion can be described by a relation such as $\sqrt{J_2} - \alpha I_1 = 0$, where J_2 is the second invariant of the stress tensor, and I_1 is the mean stress. However, failure is reached more easily when the two largest main compressive stresses are larger than the mean stress — a situation often met at a cavern wall. Before short-term failure is reached, the sample experiences dilatancy (volume increase). It has been suggested that the onset of dilatancy characterizes the long-term strength of the rock.

1.2. Mechanical Behavior of a Salt Cavern

The general outline for the mechanical behavior of caverns is similar to that for a rock sample when one considers the cavern volume loss (or increase) rate, $\dot{V}/V$, instead of the sample strain-rate, $\dot{\varepsilon}$, and when one considers the difference (or $P_\infty - P_c$) between the overburden (or geostatic) pressure (or P_∞) and the cavern pressure (or P_c) instead of the mechanical load, σ , applied to a rock sample. In a cavern, the mechanical loading is more severe when cavern pressure is *lower*.

Cavern pressure is said to be "halmostatic" when a central string is filled with saturated brine and no pressure is applied on the central string at the wellhead. In brine well or in a liquid or liquefied storage cavern, cavern pressure is most often close to halmostatic. In a natural-gas storage cavern, cavern pressure is lower than halmostatic (and large volume loss rates can be expected) when the gas stock is smaller.

However, there are some noteworthy differences between the behavior of a sample and the behavior of a cavern.

- The elastic behavior of a cavern immediately following any cavern pressure change is influenced both by the mechanical properties of the rock formation *and* by the cavern shape (see Paragraph 5).

- Steady-state behavior ($\dot{V}/V$ is constant.) is reached when the cavern pressure is kept constant for years; as is elastic behavior, steady-state behavior is influenced both by the mechanical properties of the rock formation *and* by the cavern shape.

- The transient behavior of a cavern is more complex than the transient behavior of a sample; in general, its effects last much longer than in a rock sample. In fact, one must distinguish between the "rheological" transient behavior (as observed during a laboratory test) and the "geometrical" transient behavior of a cavern — when cavern pressure changes, the non-uniform stress field around the cavern slowly changes from its initial distribution to its final steady-state distribution, an effect that does not exist when an uniaxial test is performed on a rock sample. These two transient effects combine in a cavern: the geometrical transient behavior is responsible for the very long duration of the transient phase in a cavern (see Appendix A).

- Transient "reverse" creep (i.e., cavern volume *increase*) is observed after a rapid pressure build-up (as performed, for example, at the beginning of an MIT test).

- Cavern failure is a complex phenomenon that depends on cavern size (Overbrining often results in very large caverns with roofs that cannot bear the weight of the overburden.), cavern shape, insoluble distribution in the rock mass, etc. Cavern failure is more likely to occur when the cavern pressure is much lower than the overburden pressure, a situation sometimes encountered in deep natural-gas storage caverns. However, in addition to low pressure, a rapid pressure-decrease rate is considered to be influential.

- In general, no tensile stress appears in a salt cavern, except when cavern fluid pressure is quite low and when the cavern roof is flat or the cavern shape is irregular (blocks may fall). When a cavern is submitted to a fluid pressure higher than geostatic (hydrofracturing) , fluid pressure is higher than the minimal stress at cavern wall, and fracturing may take place.

1.3. A General Comment on *In Situ* Mechanical Tests

In most cases, it is difficult to measure cavern shape or volume changes directly. In fact, during most mechanical tests, what is measured is the evolution of the wellhead pressure (in a closed cavern) or the flow rate of the expelled volume (from an opened cavern). The evolution of these quantities is influenced not only by purely mechanical effects; factors such as cavern brine warming (or cooling), additional

dissolution, brine micropermeation through the cavern walls and fluid leaks through the casing also play roles. In many cases, for instance, the effects of cavern brine warming are more significant than the effects of cavern creep closure. For this reason, interpreting an *in situ* "mechanical" test is often difficult.

2. COMPRESSIBILITY TESTS

2.1 Introduction

When a certain amount of liquid, v_{inj}, is injected in a closed cavern, the wellhead pressure increases by δP^{wh}, which, at first approximation, is also the cavern pressure increase. The relation between these two quantities (v_{inj} and δP^{wh}) generally is linear during a rapid test. A similar test can be performed by *withdrawing* a certain amount of liquid from a pressurized cavern. This test is simple, its cost is small and its interpretation is straightforward — if simple basic rules are observed (see Section 2.3).

An example of such a test is described in Thiel (1993); see Figure 2. The slope of the curve (injected brine volume versus brine pressure), or $\beta V = v_{inj} / \delta P^{wh}$, is called the cavern compressibility (in m^3/MPa or bbls/psi). Note that *tubing* pressure is measured as brine is injected into the *annulus*.

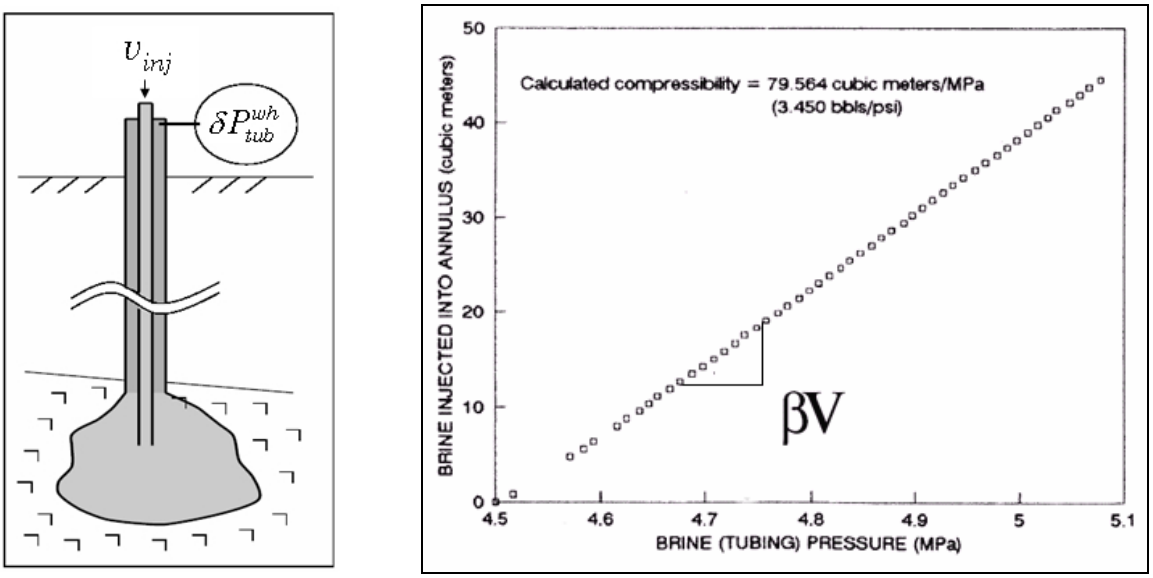

Figure 2 – Measurement of cavern compressibility. [after Thiel, 1993]

Cavern compressibility plays a significant role in various phenomena, including mechanical-integrity test design and interpretation, pressure build-up rate in a closed cavern, and blowout scenarios. Useful information on cavern volume, the existence of trapped-gas pockets, or a large insoluble volume sedimented at the cavern bottom can be inferred from a compressibility measurement.

2.2. Cavern Compressibility

2.2.1. Introduction

Cavern compressibility, or βV, can be expressed as the product of the cavern volume, V (see Section 2.2.2) and a compressibility factor, β (see Section 2.2.3). As in most cases, the cavern volume is known before the test, and the compressibility factor, at least, can be roughly estimated, the cavern

compressibility value can be predicted before the compressibility test. This is a considerable asset: any significant discrepancy between the as-measured compressibility and the predicted compressibility is a clear sign of anomalous cavern behavior (e.g., existence of gas pockets).

2.2.2. Cavern Volume

Cavern volume, V, can be estimated through sonar measurement (or injected-water mass/withdrawn- brine mass balance), but sonar measurements sometimes underestimate the actual cavern volume. This is especially true in bedded salt formations, which often contain a fair amount of insolubles. When salt is washed out, insolubles fall to the cavern bottom; with an insoluble bulking factor of the order of 1.5, brine is trapped in the sedimented insolubles. Both insolubles and trapped brine contribute to cavern compressibility, but sonar survey cannot "see" the volume of sedimented insolubles.

2.2.3. Compressibility Factor

The compressibility factor, β, is the sum of the fluid compressibility factor, β_f, and the cavern compressibility factor, β_c. During an injection, pressure in a cavern builds up by δP_c, the cavern fluid volume decreases by: $-\beta_f V \delta P_c$ and the cavern volume increases by: $\beta_c V \delta P_c$. In other words, additional room, or $(\beta_f + \beta_c) V \delta P_c$, is created to accommodate the injected volume of fluid, $v_{inj} = (\beta_f + \beta_c) V \delta P_c$ and $\beta = \beta_f + \beta_c$. In most cases, the cavern compressibility factor, β_c, is smaller than the fluid compressibility factor, β_f.

2.2.3.1. *Fluid Compressibility Factor*

When the cavity is filled with brine, $\beta_f = \beta_b = 2.7 \times 10^{-4}$/MPa. When two fluids are contained in the cavern (say, hydrocarbon and brine), the global fluid compressibility is a combination of the compressibility of the two fluids. Let x be the cavern volume fraction that is occupied by the fluid other than brine — i.e., if V is the cavern volume, the brine volume is $(1-x) V$ and the other fluid volume is $x V$; x varies from $x = 0$ (no hydrocarbon) to 1 (no brine). Then, the global fluid compressibility factor is $\beta(x) = \beta_c + x \beta_f + (1-x) \beta_b$. Most hydrocarbons are more compressible than brine, and the global compressibility factor, $\beta(x)$, is much larger than it should be when the cavern is filled with brine, $\beta(0) = \beta_c + \beta_b$. For instance, when propane is considered, $\beta_{prop} = 4.5 \times 10^{-3}$/MPa. (However, this figure is subject to large changes according to the composition of LPG; for pure propane, $\beta_{prop} = 2.9 \times 10^{-3}$ /MPa; smaller propane compressibility values were found during an *in situ* test described in Section 2.4.3.2), $\beta_c = 1.3 \times 10^{-4}$ / MPa (see below) and $\beta(x) = 4 \times 10^{-4} + 42.3 \times 10^{-4} x$ / MPa. Cavern compressibility in this case varies from $\beta(0) = 4 \times 10^{-4}$ /MPa (no hydrocarbon in the cavern) to $\beta(1) = 46 \times 10^{-4}$ /MPa (no brine in the cavern). Cavern compressibility is increased by a factor of ten when the cavern is filled with LPG (rather than brine).

The effect on cavern compressibility of an even small gas pocket is still more dramatic. The isothermal compressibility of gas is $\beta_g = 1/P$ when P is absolute pressure of gas at cavern depth (or γ/P when the pressure change is extremely rapid; γ is the adiabatic constant. In fact, these formula hold for a perfect gas and must be corrected when an actual gas is considered). A typical value is P = 20 MPa and $\beta_g = 0.05$ /MPa: gas compressibility is larger than brine compressibility by two orders of magnitude, and even a small fraction of gas is able to increase cavern compressibility drastically. For instance, $x = 0.01$ and $\beta(x=0.01) = \beta_c + x \beta_g + (1-x) \beta_b = 9 \times 10^{-4}$ /MPa, instead of $\beta(0) = 4 \times 10^{-4}$/MPa when the cavern contains no gas, or $x = 0$.

2.2.3.2. *Cavern Compressibility Factor*

The cavern compressibility factor, β_c, depends upon both cavern shape and rock-salt elastic properties (Young modulus, E, and Poisson ratio, ν). For a perfect sphere (the less compressible shape of a cavern),

$\beta_c = 3\,(1+\nu)\,/\,2E$; for a perfect cylinder, $\beta_c = 2(1+\nu)\,/\,E$. Larger values can be obtained when the cavern is "flat". Boucly (1984) suggests $\beta_c = 1.3 \times 10^{-4}$/MPa ($9 \times 10^{-7}$/psi) for the Etrez gas-storage caverns operated by Gaz de France. Slightly smaller values are suggested for the Tersanne site caverns.

Thus, a typical value of the compressibility factor of a brine-filled cavern is

$$\beta = \beta_b + \beta_c = 4 \times 10^{-4}\text{/MPa} = 2.8 \cdot 10^{-6}\text{/psi} \quad \text{(Boucly, 1984).}$$

For the case of the Manosque storage site, Colin and You (1990) propose

$$\beta = 5 \text{ x } 10^{-4}\text{ /MPa} = 3.4 \times 10^{-6}\text{/psi.}$$

For the caverns of the Total-operated Vauvert site in southeastern France, You *et al.* (1994) have measured values scattered between $\beta = 3.2$ to 8.5×10^{-4}/MPa. (Caverns are very deep, and salt content is variable.) Thiel (personal communication, 2004) suggests that $\beta = 2.94 \times 10^{-6}$/psi ($4.2 \text{ x } 10^{-4}$/MPa) works well as a "starting point". According to Blair (1998), "compressibility of the brine filled cavern can be approximated at the compressibility of brine," or $\beta = 3 \times 10^{-6}$ /psi ($4.3 \text{ x } 10^{-4}$/MPa).

2.3. Uncertainties in Compressibility Measurements

A compressibility test consists of injecting (or withdrawing) a given amount of liquid (say, brine) and measuring the subsequent change in wellhead pressure. However, note that:

(a) the change in wellhead pressure (the quantity actually measured) may differ from the change in cavern pressure (the quantity of primary interest); and

(b) several phenomena other than the elastic properties of the cavern generate pressure changes, possibly leading to misinterpretation of the test, especially when the test duration is long and/or when pressure changes during the test are large.

2.3.1. Changes in Column Composition

Cavern pressure (P_c) equals wellhead pressure (P^{wh}) plus the weight of the liquid column in the well ($\rho g H$); ρ is the fluid density of the well in kg/m^3, g is the gravity acceleration constant ($g = 10$ m/s^2) and H is the cavern depth (in m). For example, when the central tube is filled with saturated brine,

$$P_c \text{ (MPa)} = P_{tub}^{wh} \text{ (MPa)} + \rho_b g H = P_{tub}^{wh} \text{ (MPa)} + 0.012 H \text{ (m)}$$

or

$$P_c \text{ (psi)} = P_{tub}^{wh} \text{ (psi)} + 0.52 H \text{ (ft)}$$

During injection, liquid density in the well may change. Assume that, during a compressibility test, the density of the injected brine is slightly lower than the density of the brine contained in the central tube (Figure 3). Injected brine density, or ρ_{unsat}, is such that $\rho_{unsat} = \rho_{sat} - \delta\rho$. When a volume, v_{inj}^{tub} , is injected in the central tube, the following happens.

1. The cavern pressure changes by $\delta P_c = v_{inj}^{tub} / \beta V$. The annular space wellhead pressure changes by exactly the same amount, $\delta P_{ann}^{wh} = \delta P_c = v_{inj}^{tub} / \beta V$, because the annular space experiences no change in liquid composition during the brine injection. (Brine is injected into the central tube.)

2. The saturated-brine/unsaturated-brine interface in the central tube (with cross-sectional area S) drops by $h_i = v_{inj}^{tub} / S$, and the column weight in the central string changes by $\delta\rho g\, h_i = \delta\rho g\, v_{inj}^{tub} / S$, resulting in an additional change in the central tube wellhead pressure, $\delta P_{tub}^{wh} = v_{inj}^{tub} / \beta V + \delta\rho\, g\, v_{inj}^{tub} / S$.

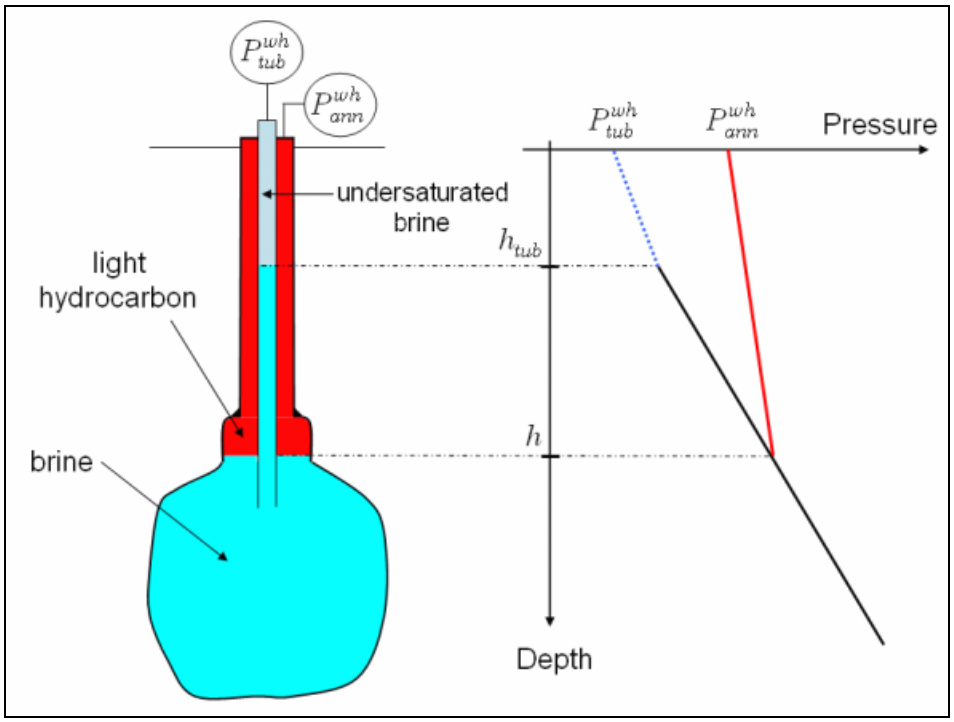

Figure 3 – Injection of under-saturated brine in the central tubing. To avoid misinterpretation, pressure evolutions must be measured in the annular space, rather than in the central tubing, $\beta V = v_{inj}^{tub} / P_{ann}^{wh}$.

In other words, during a compressibility test, when brine is injected into the central tube, pressure changes must be measured in the annular space (whose composition does not change during the test) rather than in the central tube. Conversely, when liquid is injected into the annular space, pressure changes must be measured in the central tubing. Even when undersaturation is small, large underestimation of the cavern compressibility can be made by measuring the pressure variations in the wrong tube — i.e., in the tube in which liquid was injected. Assuming, for example, that βV = 40 m^3/MPa, S = 10 liters/m (100 cm^2), $\delta\rho$ = 20 kg/m^3 and g = 10 m/s^2,

$$\delta P_{wh}^{ann}\ (\text{MPa}) = v_{inj}^{tub} / \beta V = 0.025\, v_{inj}^{tub}\ (\text{m}^3)$$

$$\delta P_{wh}^{tub}\ (\text{MPa}) = v_{inj}^{tub}\ (1 / \beta V + \delta\rho\, g / S) = 0.045\ v_{inj}^{tub}\ (\text{m}^3)$$

and the error made when measuring tubing pressure variations (instead of annular pressure variations) is 80%. Brine undersaturation can be detected readily when comparing the evolutions of the annulus and central tube pressures (see Figure 4, Note 4; after Thiel and Russel, 2004.)

Cold brine injection also induces changes in brine temperature distribution, as, at a given depth, colder brine is substituted for the warmer brine that filled the well before the test. Such an injection results in a heavier column. However, brine rapidly warms in the well to regain thermal equilibrium. Here, again, measuring pressure changes in the undisturbed annular space prevents most misinterpretations.

2.3.2. Other Effects

The above-mentioned effect (column composition changes) is by far the biggest source of misinterpretation, but there are many other effects. The cavern and the hole are the seat of various phenomena that may induce some changes in pressure evolution. Drawing a comprehensive list is difficult, and quantifying the various effects is more difficult still (see Van Sambeek *et al*., 2005). These effects include ground temperature and atmospheric pressure variations, brine permeation through cavern walls, cavern brine warming, additional dissolution and transient creep, among others. Fortunately, most of these effects are negligible in the context of a rapid test when the overall pressure change experienced during the compressibility test is not very large. When pressure changes are large and slow, additional dissolution and transient - creep must be taken into account when interpreting the test. This is especially true when brine is *withdrawn* from the cavern (see for instance Figure 4, p.7 in Clerc-Renaud and Dubois, 1980).

2.4. Examples

2.4.1. Cavern Pre-Pressurization Before a Nitrogen Interface Test

When a Nitrogen Interface Test is to be performed, it is often necessary to inject some brine in the cavern before injecting nitrogen in order to "pre-pressurize" the cavern. Let v_g be the volume that will be occupied by the nitrogen during the test: it is the sum of the annular space volume (from wellhead to casing shoe) plus the volume between the casing shoe and the nitrogen/brine interface in the cavern neck ; v_b is the volume of brine to be injected to "pre-pressurize" the cavern. Let the selected test pressure be P_{tub}^{wh} (which is the wellhead pressure as measured at the wellhead in the brine-filled central tube). Thus, the brine volume to be injected, v_b, is such that $v_g + v_b = \beta V \, P_{tub}^{wh}$. For instance, in a 80,000-m^3 cavern at a 1000-m depth, reasonable values are $\beta V = 40$ m^3/MPa, $P_{wh}^{tub} = 15$ MPa and $v_g = 50$ m^3, and the amount of brine to be injected before injecting nitrogen is:

$$v_b = 40 \text{ x } 15 - 50 = 550 \text{ m}^3.$$

As a consequence of brine injection, wellhead pressure builds by:

$$P_{tub}^{wh} = v_b / \beta V = 13.75 \text{ MPa}$$

In addition, gas injection will result in an additional wellhead pressure build-up by:

$$P_{tub}^{wh} = v_g / \beta V = 1.25 \text{ MPa}$$

2.4.2. Interpretation of a (Liquid-Liquid) Mechanical Integrity Test

In a Pressure Observation Test (Thiel and Russel, 2004), cavern pressure is built up at the beginning of the test (Figure 4). After a stabilization period of a few days, the pressure decay rate (in psi/day, or MPa/day) is computed. The pressure decay rate must be converted into an apparent leak rate. This is obtained readily by multiplying the pressure decay rate (Figure 5) by the cavern compressibility:

$$Q = \beta V \ \dot{P}_{tub}^{wh}$$

For this reason, cavern compressibility must be measured carefully during the initial pressure build-up before the test (Figure 4).

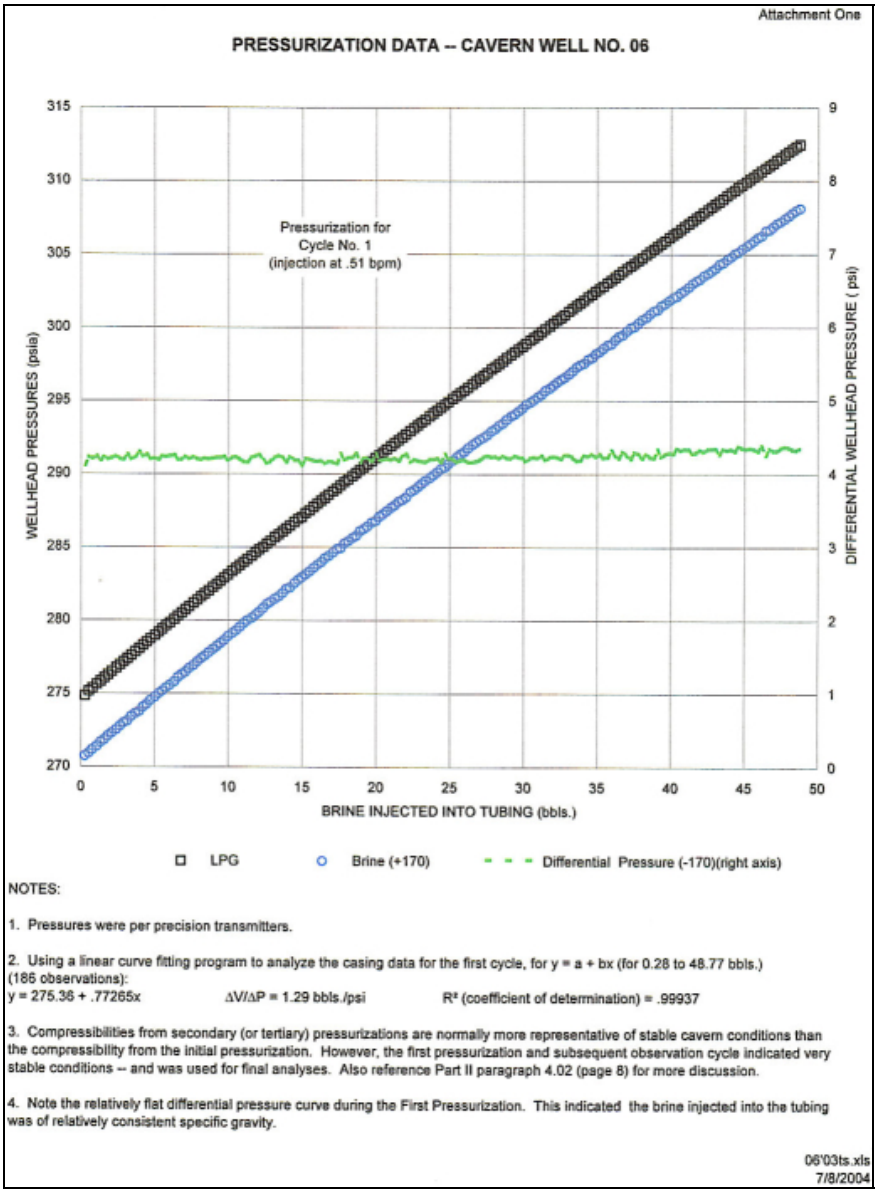

Figure 4 – Cavern compressibility, or βV , was measured at the end of the pressurization period before an MIT was performed (after Thiel and Russel, 2004).

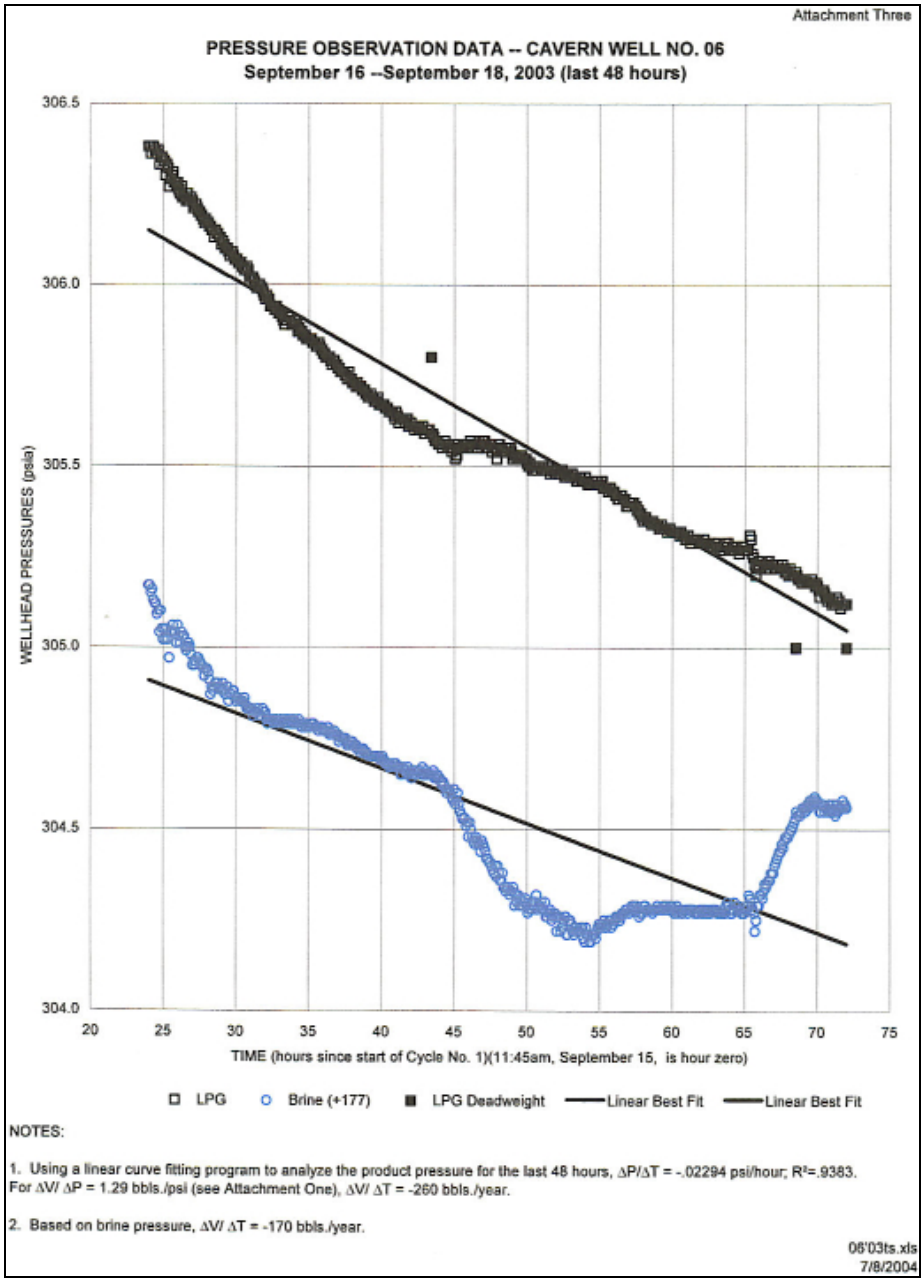

Figure 5 – During the last 48 hours of the test, the average pressure-decay rate is measured. It is converted into an apparent leak rate by multiplying the pressure-decay rate by the cavern compressibility. As βV = 1.29 bbls/psi and $\dot{P}_{ann}^{wh}$ = -0.02294 psi/hour, the (apparent) leak is Q = - 0.0296 bbls/hour = - 260 bbls/year (after Thiel and Russel, 2004).

2.4.3. Blow-Out Scenario

2.4.3.1. *Introduction*

Complete failure of the wellhead is highly unlikely. However, from the perspective of risk analysis, it is important to evaluate the volume of liquids that would be released from the cavern upon total decompression following a hypothetical complete wellhead failure (Figure 6). Consequences would be most severe in the case of LPG storage, as LPG density is low while its compressibility is large.

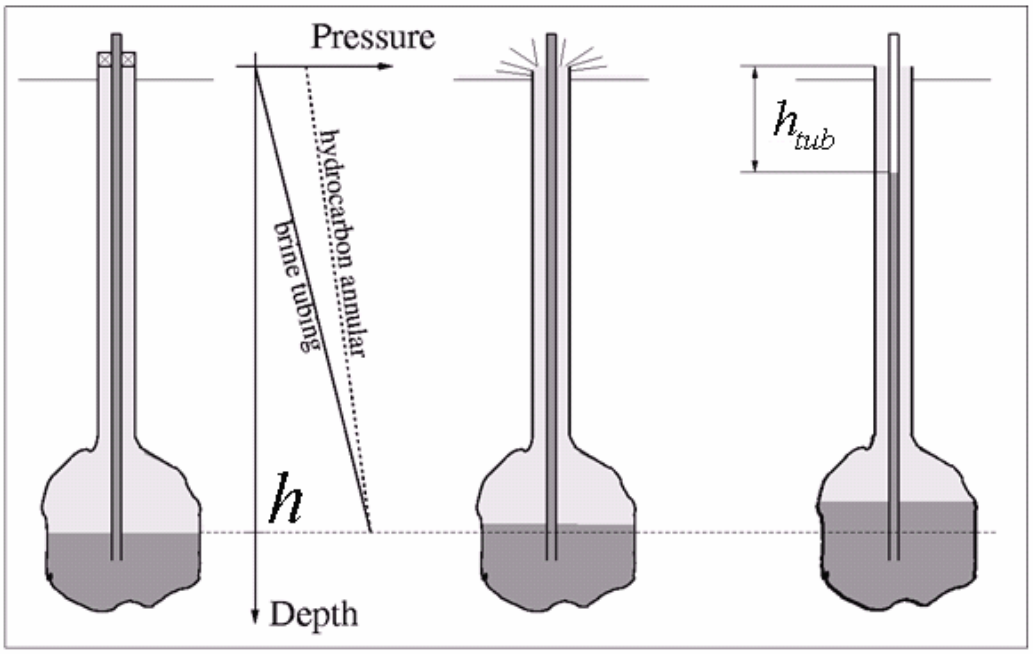

Figure 6 - Scenario of a blow out: When the valve fails at ground level, liquid is expelled until a new equilibrium is reached, and the air/brine interface in the central tubing drops by h_{tub}. The amount of expelled hydrocarbon is proportional to cavern compressibility.

If ρ_h is the hydrocarbon density (say, ρ_{prop} = 500 kg/m^3 when propane storage is considered) and ρ_b is the brine density (ρ_b = 1200 kg/m^3), the hydrocarbon pressure at the wellhead (when brine pressure at the wellhead is zero) is a linear function of brine/hydrocarbon interface depth or h:

$$P_{ann}^{wh} = (\rho_b - \rho_{prop})gh \text{ or } P_{ann}^{wh}(\text{MPa}) = 0.007h \text{ (m)}$$

or

$$P_{wh}^{ann}(\text{psi}) = 0.3\ h \text{ (ft)}$$

After failure of the wellhead, the hydrocarbon pressure at the wellhead drops to zero, and the brine level in the central tube falls to a depth, h_{tub} , such that the weight of the two fluid columns (brine and hydrocarbon, respectively) are equal at interface depth:

$$h_{tub} = h(\rho_b - \rho_{prop})/\rho_b$$

or h_{tub} = 0.58 h. The pressure drop is P_{ann}^{wh}, and the hydrocarbon volume expelled is due mainly to decompression of cavern fluid:

$$v_{\exp} = \beta V P_{ann}^{wh} = \beta V(\rho_b - \rho_{prop})gh$$

(Note that, in addition to decompression of cavern fluid, a volume Sh_{tub} is expelled because of interface drop in the central tubing. This additional volume is small, for instance h = 480 m, h_{tub} = 280 m and Sh_{tub} = 2.8 m^3 when tubing cross sectional area is S = 10 liters/m). Cavern compressibility, or βV , is higher when the amount of hydrocarbon in the cavern is larger, as hydrocarbons are more compressible than brine (see Section 2.2.3.1).

2.4.3.2. Example

The SPR1 cavern in the Carresse site was operated until 2002 by the Total Company to store propane. The casing-shoe depth is 348 m below ground level; the cavern-bottom depth is 381.5 m. The cavern volume is 13,000 m^3 (as measured in 1992). The brine/propane interface depth is approximately h = 365 m. (In fact, interface depth is a function of propane content; however, as the cavern height is small, no attempt is made here to take into account the relatively small variations in interface depth.)

In the case of wellhead failure, the cavern pressure would drop by

$$P_{wh}^{ann} = (\rho_b - \rho_{prop})gh = (1200 - 500) \times 10 \times 365 = 2.5 \text{ MPa.}$$

The amount of expelled hydrocarbon depends upon cavern compressibility.

Compressibility measurements were performed at three different periods (Figure 7). Cavern compressibility (βV) was measured during brine injection (pressure measurement resolution = 500 Pa). Assuming reasonable values of the compressibility factor (which is a function of propane content, $\beta(x) = \beta_c + x\,\beta_{prop} + (1-x)\,\beta_b$; see Section 2.2.3.1), the propane volumes in the cavern (or xV) were back-calculated; they were in good agreement with operator's data, which were obtained through surface flowmeters, providing confidence in measurement results.

Thus, it was possible to assess the amount of liquid propane, or $v_{\exp} = \beta V P_{wh}^{ann}$, that would be expelled upon total decompression by P_{wh}^{ann} = 2.5 MPa:

- when the propane volume is 700 m^3, v_{exp}= 9 x 2.5 = 22.5 m^3;
- when the propane volume is 7800 m^3, v_{exp}= 24 x 2.5 = 60 m^3; and
- when the propane volume is 10,800 m^3, v_{exp}= 35 x 2.5 = 87.5 m^3.

2.5. Dynamic Compressibility Tests

In addition to brine or hydrocarbons, the cavern, the casing or the strings are elastic bodies. When they are affected rapidly by small changes in pressure or shape, these bodies vibrate according to their mechanical properties, sizes, shapes and mechanical interactions. These vibrations constitute an important source of information (Bérest et al., 1999).

The following example is provided by the period of waves in the central tube. In brine-production wells, especially when salt is leached out from a bedded-salt formation, insoluble blocks occasionally fall to the cavern bottom and may break the central tube, whose subsequent exact length becomes unknown. In fact, tubing length can be assessed readily by measuring the periods of stationary waves.

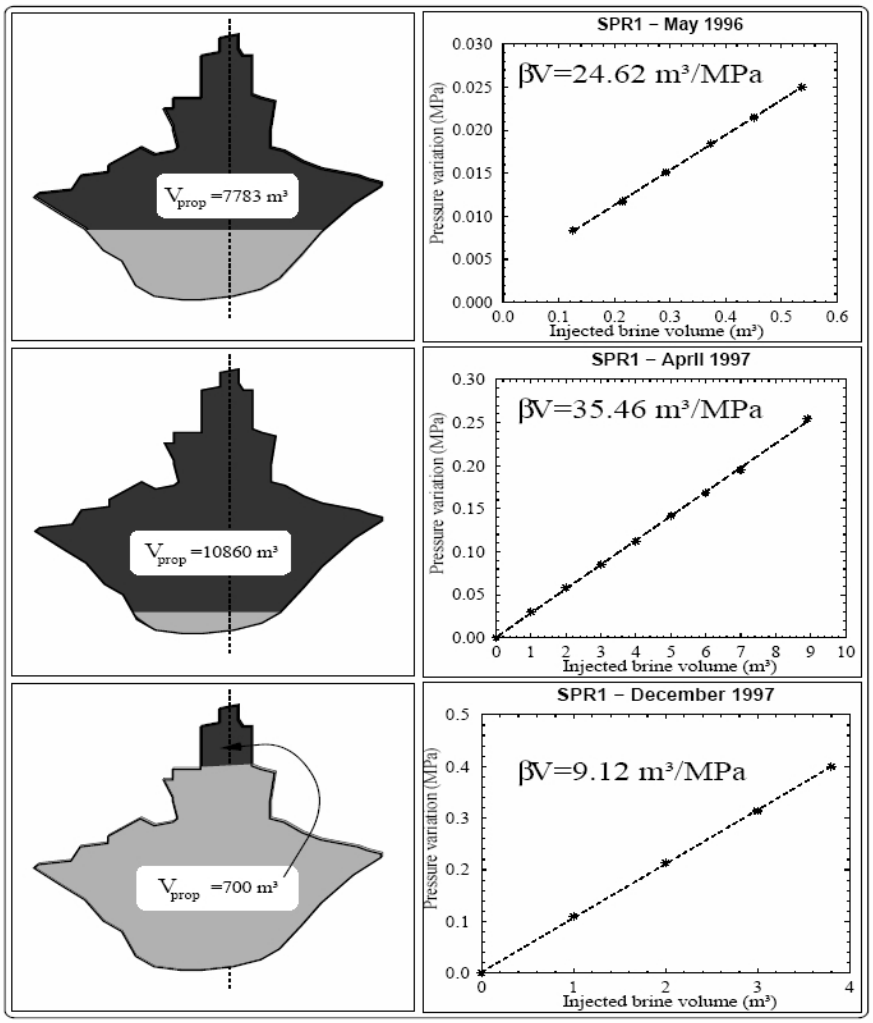

Figure 7 – Three cavern compressibility measurements for the Carresse SPR1 Cavern: Propane is much more compressible than brine; cavern compressibility is greater when the volume of stored propane increases (Bérest et al., 1999) .

Example — A cavern is slightly pressurized, and a valve is opened rapidly and then closed to generate a "water hammer". In the process of opening and closing the valve, a few liters of brine are withdrawn from the central tube. Stationary waves develop in the liquid-filled tube and dissipate slowly (Figure 8). The liquid flow rate is zero at the wellhead, and the liquid pressure (which remains equal to cavern brine pressure) is constant at the tubing shoe. The waves are "quarter-waves" whose periods (T) are related to tubing length (H) and wave speed in the well (c) through the relation $c\ T = 4\ H$. The period, T, can be assessed through data processing with an accuracy of $\delta T/T = 10^{-3}$, allowing, in principle, H to be back-calculated. However, wave speed in the tube, or c, becomes a problem. The speed depends both on wave speed in the liquid (c_b = 1800 m/s, when brine is considered) and tubing compressibility. Wave speed in the tube always is slower than wave speed in the liquid; c = 1000 m/s is typical, and the period of stationary waves is close to 4 sec in a tube that is H = 1000-m long. Good results are obtained when a reference measurement is available for comparison. (For instance, c can be measured at the beginning of the leaching process when the tubing length, H, is known.) Then, any change in the value of T can be converted readily to a change in the value of H. A fundamental requisite, however, is that the composition of the liquid column remain identical from one test to another: the value of c must remain unchanged.

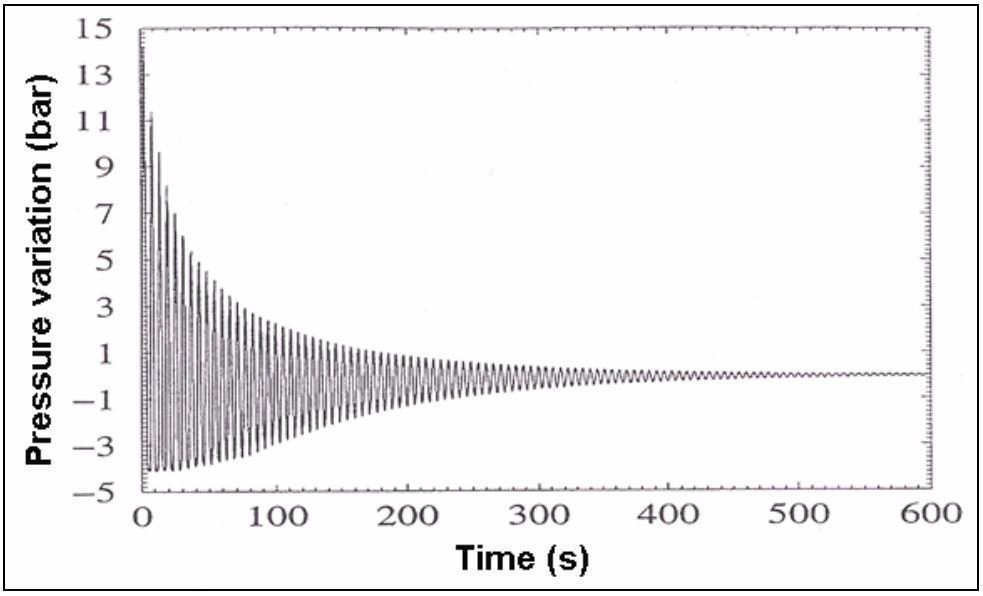

Figure 8 - Quarter-waves in the tubing during a test at Vauvert facility: A valve is opened and closed rapidly at the beginning of the test; wellhead pressure as a function of time is measured; tubing length is back-calculated from the stationary wave period.

3. CAVERN CREEP CLOSURE: SHAPE-CHANGE MEASUREMENT

3.1. Introduction

All solution-mined caverns converge as they gradually, and quite slowly, shrink. The driving force for such convergence is the difference between the overburden pressure (P_∞) and the cavern fluid pressure at cavern depth (P_c). The rate of cavern convergence is faster in a deeper cavern (When cavern depth increases by a factor of two, convergence rate increases by one or two orders of magnitude, because the difference $P_\infty - P_c$ is larger; warmer rock temperature at greater depth also is influential.); at a given depth, the convergence rate in a natural-gas storage facility is much faster when the gas pressure is minimum than it is in a brine-filled cavern when pressure is halmostatic.

Convergence rates in shallow, fluid-filled caverns are slow. Brouard (1998) measured brine outflow from a 950-m deep, 8000-m^3 cavern as 7.2 l/day, or $\dot{V}/V = -3\times10^{-4}$ /year — a very small figure. Conversely, some natural-gas storage facilities have experienced large losses of volume. According to Baar (1977, p.143-144), who studied the 2000-m deep Eminence salt-dome cavern (Mississippi), "The unexpected anomalies in the closure of the first cavern included a rise in the cavity bottom by 120 ft (36 m) and a cavity storage loss possibly up to 40%." (see Figure 9). These anomalies were observed after a 2-year long period during which gas pressure had been lowered over several months to 1000 psi (7 MPa). Boucly (1984) provides data on Te02, a 90,000-m^3 cavern at a depth of 1450 m. This natural-gas storage cavern experienced low gas pressures from 1970 to 1980. After nine years of operation, the volume available to gas had decreased by about 35% (see Figure 9). The Kiel case is described in Section 4.5.3.

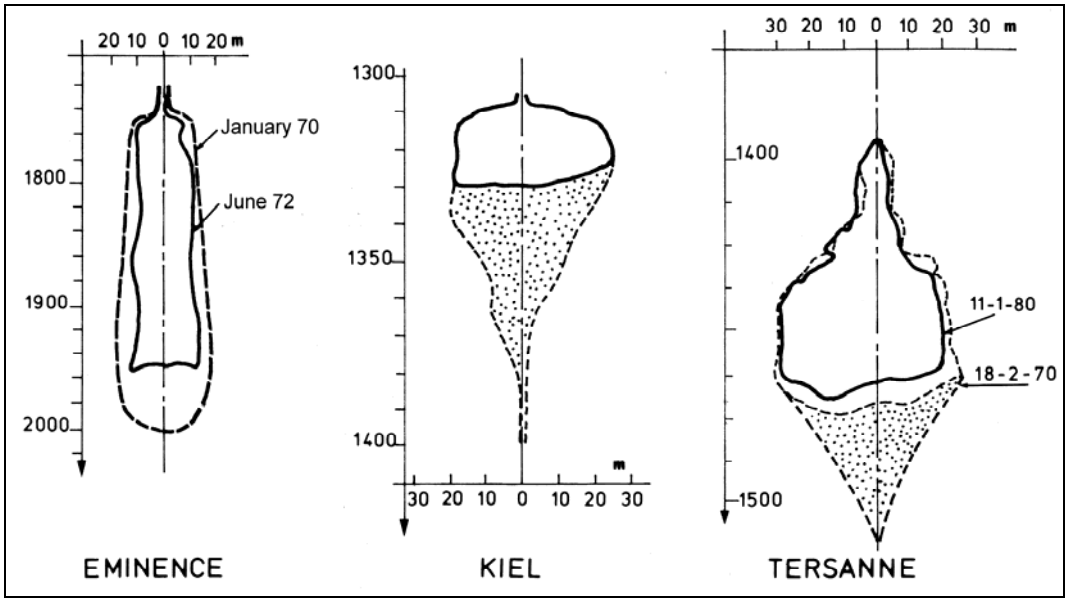

Figure 9 - Creep closure at Eminence (Mississippi), Kiel (Germany) and Tersanne (France): The dotted surfaces represent insolubles sedimented at the cavern bottom. Depths are in meters. Volume losses for the Kiel cavern are not represented.

3.2. Measurement of Cavern Shape

3.2.1. Sonar Survey

Direct inspection of a cavern is impossible, but sonar surveys allow the shape of a cavern to be measured. In a brine-filled cavern whose shape is regular, accuracy of a few percent can be obtained. In other words, only relatively large changes in cavern shape and volume can be measured accurately through sonar surveys. Sonar surveys are quite effective during cavern washing, as, during this period, the cavern radius or height may change by several, or dozens of, meters. When leaching is completed, much slower evolution is expected, and, in most cases, sonar surveys are not accurate enough to detect changes in cavern shape. One outstanding exception can be found in the case of deep natural-gas storage caverns, as some of these caverns have experience large volume changes (see Section 3.1). However, performing a (standard) sonar survey requires refilling the cavern with brine, a relatively costly and time-consuming operation. For the Tersanne and Eminence caverns, mentioned above, the volume changes were large enough that performing a sonar survey was useful (Figure 9).

Quast and Schmidt (1983) describe a slender 400,000-m^3 cavern (1000 m to 1280 m in depth). After 4 years of gas-storage operation during which the cavern pressure varied between 2.5 MPa and 16 MPa, a "modified" sonar survey was performed. It was found that the cavern had "not undergone any substantial changes within the limits of measurement accuracy…and convergence rates remain lower than a quantifiable magnitude of several percent" (Quast and Schmidt, 1983, p.218-219 and Figure 2).

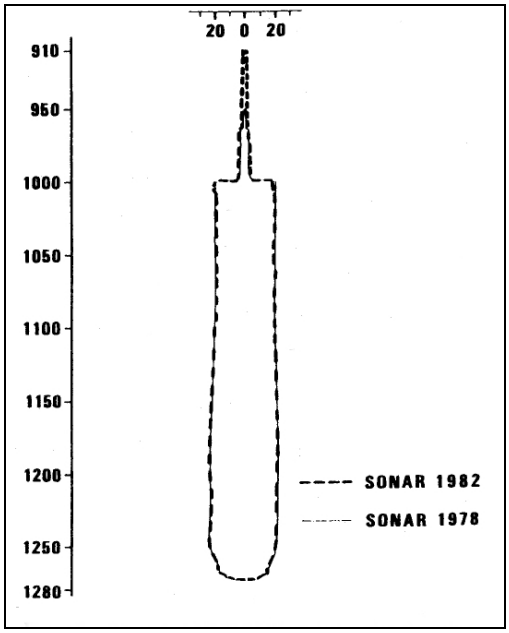

Figure 10 – Comparison between sonar surveys performed in 1978 and 1982: Depth and radius are in meters (after Quast and Schmidt, 1983).

3.2.2. Gas Sonar Survey

Deep gas-filled caverns are a concern: on one hand, they are prone to develop large convergence; on the other hand, a standard sonar survey cannot be performed in a gas-filled cavern. Gas sonar methods have been developed to measure the shape of a gas-filled cavern. One such case is described in Quast and Schmidt, 1983, Figure 3; another can be found in Cole (2002). Caverns #2 and #5 are operated as gas-storage caverns at the Markham Storage Field in southern Texas. The depth of Cavern #2 was 3450 ft to 5189 ft by June 1992, when it first was filled with gas; its displaced volume was 4 MMbbls. The corresponding figures for Cavern #5 were 3531 ft to 5815 ft by October 1995; the displaced volume was 3.44 MMbbls.

The caverns were cycled 8 to 10 times each calendar year. Each year, total-depth and brine-gas interface surveys were run on each cavern. As of January 2002, Cavern #2 and Cavern #5 had lost 292 ft and 419 ft of cavern depth, respectively. Assuming that cavern shape had not changed since the time that sonar surveys had been conducted before the first gas injection (In other words, volume change is assumed to result from bottom upheaval; no other possible shape change is considered.) allows the "apparent" volume loss to be assessed. However, it was suspected that both storage-volume loss and salt sluffing from the walls and roof had taken place. (Salt sluffing results in a rise in total depth and brine interface but no net loss of usable volume.) A material balance test confirmed that salt sluffing accounted for at least some part of the cavern height loss. (As a known amount of gas was withdrawn from each cavern and the pressure and temperature were measured before and after withdrawal, the cavern volume can be assessed using the gas state-equation; see Section 3.3.)

At this point, it was decided to conduct a gas sonar survey, and the hanging pipe was cut at the roof of the cavern. The gas sonar measurement run gave a cavern volume that compared closely to the calculated material balance volumes. The apparent loss of space occupied by the natural gas as of the start of operations to May 2001 was a combined 0.857 MMbbls — in fact, the actual loss in space volume was adjusted to 0.413 MMbbls (attributable to cavern creep closure), the difference (or 0.444 MMbbls) resulting from salt falling from the upper part of the caverns and filling the lower part of the caverns.

3.3. Measurements of Cavern Volume

3.3.1. Gas cavern

Sonar surveying is the most accurate method for assessing cavern volume and volume evolution, but it is difficult to perform and interpret sonar surveys of natural-gas storage caverns. Performing a standard sonar survey requires filling the cavern with brine — a costly process. Thus, various attempts have been made to use natural gas inventory to assess cavern loss in gas-filled caverns.

The mass of gas contained in a cavern, or m, can be calculated from the gas equation (see Nelson and Van Sambeek, 2003):

$$PV = mZRT$$

where P = gas absolute pressure,

V = cavern volume,

Z = gas compressibility factor,

R = gas constant, and

T = gas (absolute) temperature.

P and T can be measured, and Z is a known function of P and T — in other words, when m (gas mass) is known (through gas-injection/withdrawal metering), V, or the cavern volume, can be back-calculated. (In a tall cavern, T and P are functions of depth; temperature distribution as a function of depth, or $T=T(z)$, can be measured through a temperature log; the mechanical equilibrium equation, or $dP/dz = \rho g$, together with the gas equation, can be integrated with respect to depth to compute pressure distribution.)

Hence, in principle, accurate metering of injected/withdrawn gas masses allows cavern volume evolution to be assessed as a function of time. However, metering errors cannot be avoided, and small errors accumulate over time, leading to large uncertainties.

When the gas mass is poorly known, as is the case after the cavern experienced several withdrawal/injection cycles, a known quantity of gas, or $m_2 - m_1$, can be injected (or withdrawn). Measuring pressures and temperatures before (P_1, T_1) and after (P_2, T_2) the injection (or withdrawal) allows to the cavern volume to be back-calculated:

$$m_2 - m_1 = \left(\frac{P_2}{Z_2 R T_2} - \frac{P_1}{Z_1 R T_1} \right) V$$

Here, again, uncertainties must be assessed (Nelson and Van Sambeek, 2003).

Cavern volume can also be assessed through chemical tracing. A description of this method can be found in a 1987 Gaz de France SMRI Report. In chemical tracing, a gas sample is collected in the cavern prior to the test to measure the initial concentration of the tracer gas, a known quantity of which then is injected into the cavern. The best tracer gas is hydrogen, as hydrogen diffusion through any other gas is extremely fast. After the tracer gas has become mixed sufficiently, a second gas sample is collected, and the tracer-gas concentration is measured. The increase in gas concentration allows the cavern volume to be computed. Gaz de France (1987) reports the uncertainty in estimating cavern volume with chemical tracing to be about 2%.

These three methods: gas inventory and temperature log, effect of a gas injection (or withdrawal) and chemical tracing, are illustrated in Figure 11.

3.3.2. Oil cavern

In the case of oil storage caverns, comparison between "…calculated solution volumes based on dissolution of salt by raw water, calculated sonar volumes based on the sonar surveys of the cavern dimensions and cavern volumes occupied by metered oil inventories…" can be found in Munson and Myers (2000).

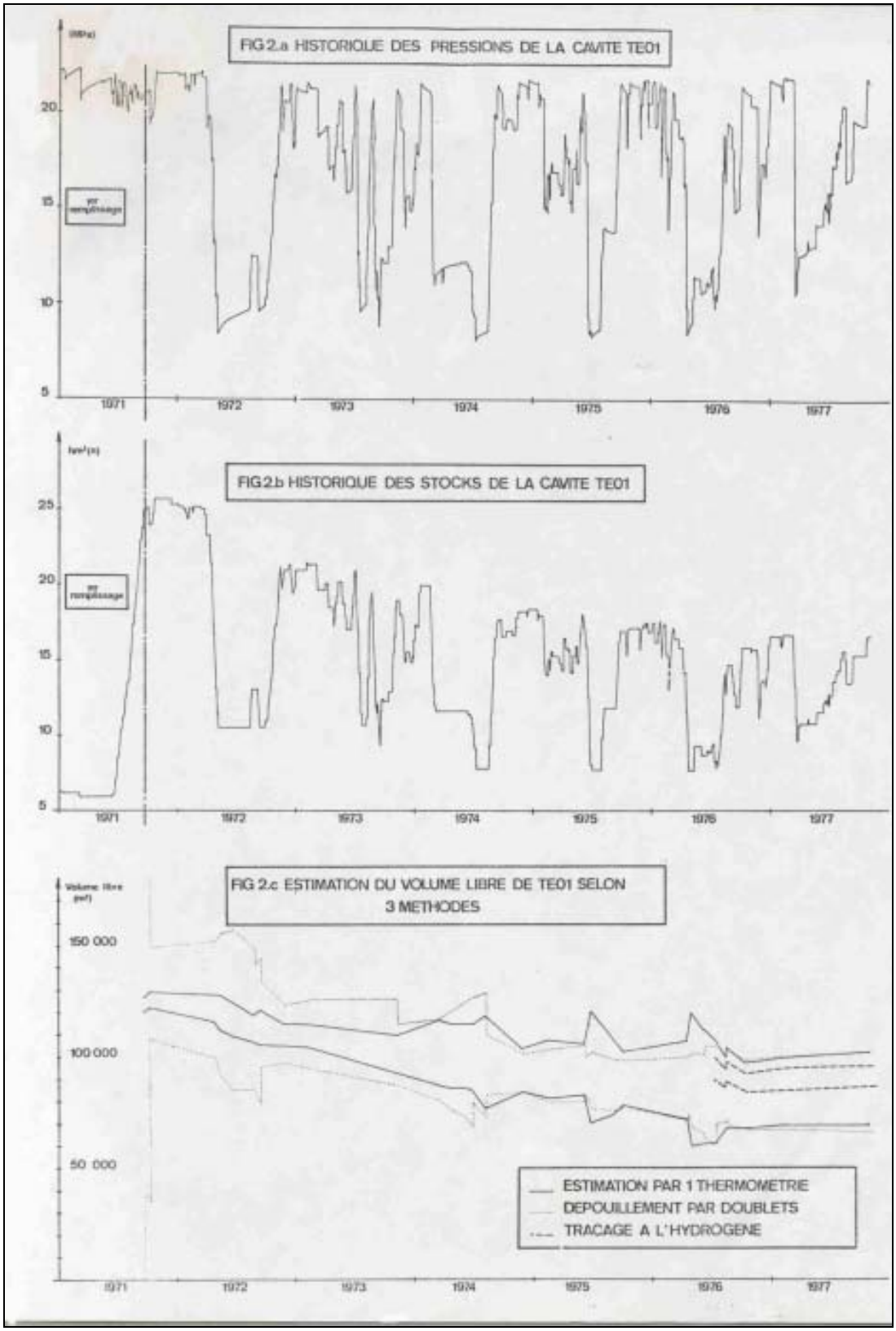

Figure 11 – The Tersanne 01 cavern, operated by Gaz de France, leached out by 1971: Cavern-pressure (in MPa) history and gas-inventory history (in Mons Nm^3) strongly suggest that a significant loss of cavern volume occurred during 1971-1976. The usable cavern volume was estimated by (a) measuring gas mass and gas temperature ("estimation par un thermomètre"), (b) withdrawing or injecting a known quantity of gas ("dépouillement par doublets"), and (c) hydrogen tracing ("traçage à l'hydrogène").

4. SHUT-IN PRESSURE TESTS AND EXPELLED FLOW-RATE TESTS

4.1. Introduction

The cavern-creep closure rate can be assessed through shut-in pressure tests and expelled flow-rate tests. Both tests can be performed in liquid-filled caverns.

Shut-in pressure tests consist of closing the cavern and measuring the pressure evolution at the wellhead as a function of time. It is better (by far) to measure the pressure evolution in both the annular space and in the central tube to provide redundancy and to assess casing leaks.

Expelled flow-rate tests consist of opening the cavern and measuring the flow of fluid (brine or hydrocarbon) expelled from the wellhead. For example, the expelled volume can be collected in a container and the fluid volume or the container weight measured on a daily basis. In a small cavern, the daily flow rate is relatively small, and measurements can be taken automatically.

These tests — especially the shut-in pressure tests — are relatively easy to perform. Much data have been published in the literature (see, for instance., Bérest et al., 2000). Interpreting these tests is not straightforward: in addition to cavern creep closure, many phenomena can contribute to pressure build-up or liquid outflow. Some of these phenomena (ground temperature variations, atmospheric pressure variations, earth tides, etc.) have relatively small effects and do not lead to a systematic error (They are more or less periodic.), but other phenomena have a much larger influence. These phenomena include cavern brine warming, additional dissolution, transient creep and (especially for shut-in pressure tests) well leaks, casing leaks or brine micro-permeation through the cavern wall.

4.1.1. Brine Warming

In most cases, cavern brine warming (or cooling) has the largest effect on pressure evolution during a shut-in pressure test (or fluid outflow during an expelled flow-rate test). Except perhaps for caverns that have been kept idle over long periods of time, the fluids contained in a cavern are not in thermal equilibrium with the surrounding rock mass. Caverns often are leached out using water pumped from a river, lake or shallow aquifer, and the water is significantly colder than the rock formation at cavern depth. During leaching, a brine cavern is not provided enough time to reach thermal equilibrium. After leaching is completed, cold brine gently warms up and its volume increases (thermal expansion), and this volume increase generates pressure build-up (in a closed cavern) or brine outflow (from an opened cavern). In other words, brine warming has exactly the same effect as cavern creep closure. In fact, in most cases, the effect of brine warming is larger than the effect of cavern creep closure. A naive interpretation (i.e., disregarding thermal effects) would lead to a gross overestimation of cavern-creep closure rate. A discussion can be found in Ehgartner and Linn, 1994, or Van Sambeek *et al*., 2005.

The thermal evolution of a cavern is governed by heat transfer (Fourier equation) in the rock mass and by the nature of the fluid contained in the cavern. For a brine-filled cavern, the characteristic time associated with heat transfer is $t_c = V^{2/3} / 4k$, where k is the thermal diffusivity of salt, and V is the cavern volume. A typical value of thermal diffusivity is k = 100 m^2/year. When V = 8000 m^3, $V^{2/3}$ = 400 m^2 and t_c = 400/ (4×100) = 1 year. In a larger cavern, the characteristic time is longer (t_c = 16 years in a V = 500,000 m^3 cavern). After a time t_c-long, the initial temperature gap is divided by a factor of approximately 4. (This last figure holds when an idealized spherical cavern is considered; it is lower in a "real-life" cavern.)

This estimation holds for a brine-filled cavern. The characteristic time is shorter when the cavern is filled with liquid hydrocarbons, which have heat capacities smaller than brine's; and smaller still when the cavern is filled with natural gas.

Let θ_o be the initial temperature gap between the rock mass and the cavern brine (e.g., at the instant when leaching is completed); θ_o can be a couple of dozens of degrees Celsius (more in a deep cavern, less in a shallow cavern). The average temperature increase rate is θ_o/t_c. (In fact, this figure is an average value; the actual temperature increase rate is much faster at the beginning of the process and much slower after a time equal to or greater than t_c. However, this simple formula holds for rough estimations.)

- During a shut-in pressure test, the pressure build-up rate generated by the temperature increase is $\dot{P}_i = (\alpha/\beta)\vartheta_0/t_c$. As $\alpha/\beta \approx 1$ MPa/°C, the average pressure build-up rate due to thermal expansion in an 8000-m^3 cavern when the initial temperature gap is θ_o = 10 °C is 10 MPa/year.
- During a flow-rate test, the liquid outflow generated by the temperature increase is $Q = \alpha V \vartheta_0/t_c$, where α is brine thermal-expansion coefficient. As $\alpha = 4.4\times10^{-4}$/°C, the liquid outflow rate is 35 m^3/year (100 liters per day, or 0.6 bbl/day) in an 8000-m^3 cavern; the initial temperature gap still is assumed to be θ_0 = 10 °C.

A good example of this is provided by a test performed on the Etrez 53 cavern operated by Gaz de France. The volume of this cavern is 8000 m^3, and its depth is 950 m. It had been leached out between March 19, 1982 and July 6, 1982. In the following, July 6 is the origin of time. This cavern was kept idle for a long time, and its pressure remained constant except for a 3-month long period during which cavern pressure was lowered by 3 MPa (see Section 4.4.2). Several brine outflow tests were performed on this cavern at different times after leaching was complete (Figure 12).

During days 47 to 91, the brine outflow slowly decreased from 240 l/day to 175 l/day (Figure 12a). A second test was performed during days 253 to 358: the outflow rate during this period was approximately 55 l/day (Figure 12b). Eight years later, during days 3032 to 3068, the brine outflow was measured again, at which time it was 6 l/day (Figure 12c). Only this last value, $\dot{V}/V = -3\times10^{-4}$/year, can be considered as being representative of cavern creep closure. The characteristic time for brine warming is t_c = 1 year: 8 years after leaching was complete, the brine thermal expansion can be disregarded. The large outflow rate figures observed earlier are by no means representative of cavern creep closure: during this period, brine outflow was governed mainly by brine thermal expansion: the initial temperature gap in this cavern was 18.5 °C; the average expelled flow rate can be expected to be 185 liters/day during the first year after leaching was complete (and faster immediately after leaching ended). In other words, interpretation of a shut-in pressure test (or of an expelled flow-rate test) is only possible when the rate of temperature increase during the test can be measured and/or assessed. (The temperature increase rate is slower in a larger cavern, and accurate measurement requires a longer testing period.)

Note that in some cases (shallow caverns), the brine may be *warmer* than the rock mass at cavern depth. In such a case, brine experiences thermal *contraction* after leaching is complete, leading to a possible *underestimation* of cavern convergence.

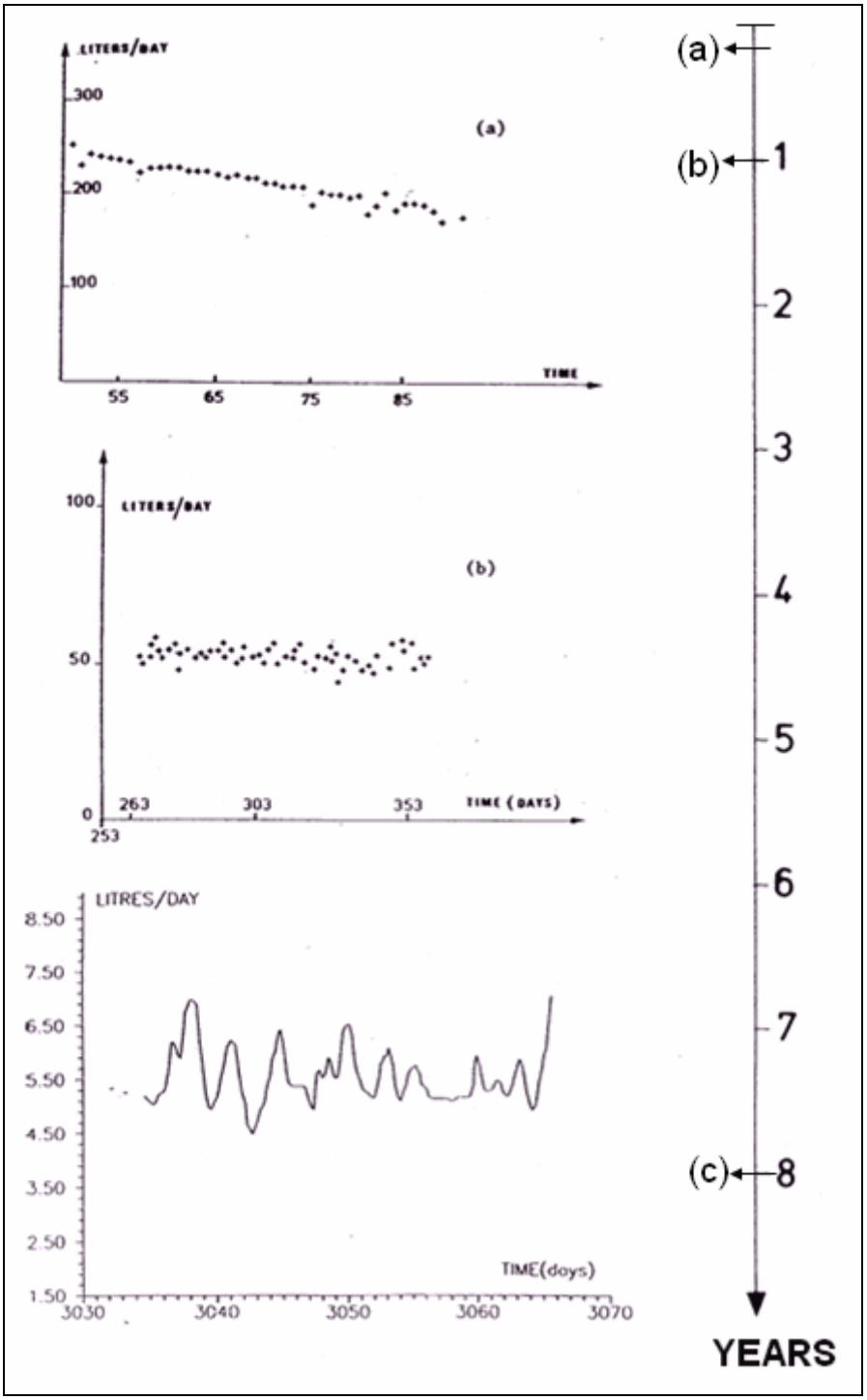

Figure 12 – An expelled brine flow test: In this 950-m deep, 8000-m^3 cavern, expelled brine flow as a function of time was measured (a) 2 months (b), one year, and (c) eight years after leaching was completed. Only the last curve (c) is representative of cavern creep closure.

4.1.2. Transient Creep

In most cases, even when a cavern has been kept idle for a long period of time (several months or years) before performing a mechanical test, steady-state creep still is far from being reached. This notion is developed through an example in Appendix A. Even when brine warming can be neglected (or is precisely known), interpretation of an *in situ* mechanical test is not straightforward. This is especially true for shut-in pressure tests, as pressure continuously varies during the test, and a complex distribution of stresses develops inside the rock mass.

4.1.3. Casing Leaks and Liquid Micro-Permeation through the Cavern Walls

Clear proof of the influence of casing leaks (and, to a lesser extent, of brine micro-permeation through cavern walls) is provided by the results of any Mechanical Integrity Test. After pressure is built up rapidly in a closed cavern, decay in wellhead pressure is observed consistently for several days and more. This effect is less significant at the beginning of a shut-in pressure test, as the cavern pressure is still close to halmostatic during this initial phase. When the cavern pressure progressively increases, possible leaks through the casing and brine micro-permeation through the cavern walls become larger and must be taken into account when interpreting test results.

Casing leaks can be estimated when pressure evolution is measured both in the brine-filled central tube and in the annular space — which should be filled with a light liquid hydrocarbon. Any hydrocarbon leak results in a differential evolution of the annular space and tubing pressures. This differential evolution can be detected easily; back-calculation of the hydrocarbon leak is straightforward if the cross-sectional area of the cavern neck is known (see Van Sambeek *et al.*, 2005).

Micropermeation effects are observed easily when brine thermal-expansion effects become negligible. A shut-in pressure test sponsored by the SMRI (Bérest *et a*l., 2001) of the Etrez 53 cavern (described above; see Section 4.2) was performed in 1996, or 14 years after the cavern was leached out (see Figure 13). After such long a period, the brine thermal expansion was complete, as the characteristic time for thermal expansion in such a cavern is t_c^{th} = 1 year (see Section 4.1.1). Two mechanisms remain active: cavern creep closure, and brine permeation through cavern walls. The former is faster than the latter when cavern pressure is high, resulting in a pressure decrease; conversely, the former is slower than the latter when cavern pressure is low, resulting in a pressure increase.

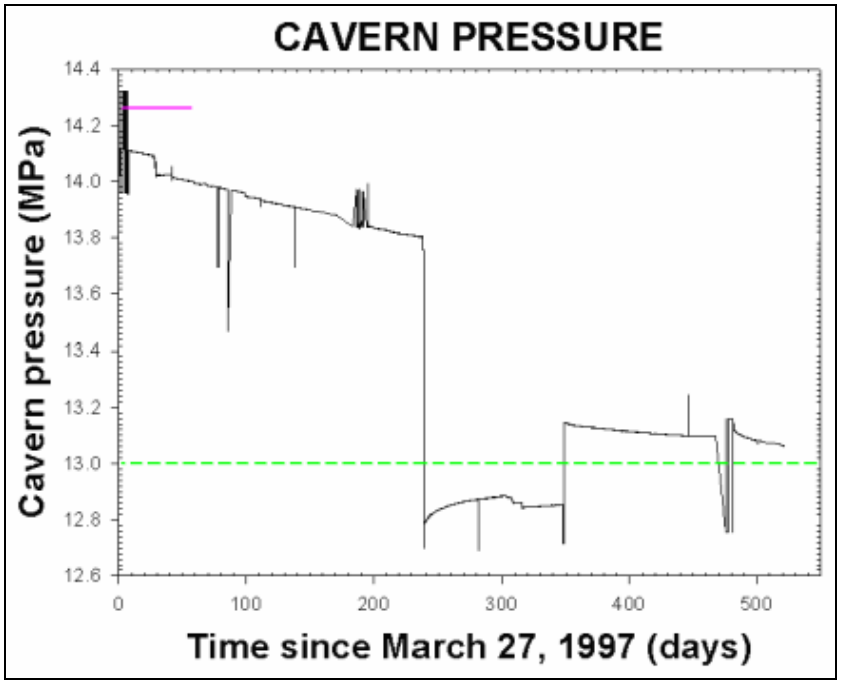

Figure 13 – This small (8000-m^3) cavern had been kept idle for 14 years before the test began. Large cavern pressure build-up (due to creep closure) is prevented by brine permeation through the cavern walls. In this cavern, halmostatic pressure and geostatic pressures are 11 MPa and 20.5 MPa, respectively (after Bérest et al., 2001).

4.2. Liquid Outflow Test

4.2.1. Brine Outflow Test

An example of the Brine Outflow Test was provided in Section 4.2 (see Figure 12).

The "brine outflow" test is simple and cost effective. However, in such a test, the central tubing (open at ground level) is filled with saturated brine; consequently, the cavity pressure is halmostatic, and the influence of non-halmostatic cavity pressure on creep closure rate cannot be investigated.

4.2.2. Hydrocarbon Outflow Test

A lower-than-halmostatic cavern pressure can be tested with a different procedure (Hugout, 1988). The annular space is filled with a light hydrocarbon (say, $\rho_h = 900$ kg/m^3). The hydrocarbon/brine interface is located in the cavern neck, below the casing shoe.

Let h be the hydrocarbon/brine interface depth in the annular space: the wellhead pressure in the annular space is $P_{wh}^{ann} = (\rho_b - \rho_h)\, g\, h$. For example, when h = 1000 m, P_{wh}^{ann} = 3 MPa. After some period of stabilization, the annular space is vented, resulting in:

(1) a hydrocarbon pressure drop of $\delta P_{wh}^{ann} = P_{wh}^{ann}$;

(2) hydrocarbon venting in the amount of $\beta V\ P_{wh}^{ann} = \beta V (\rho_b - \rho_h)\, g\, h$;

(3) and a decrease in the air/brine interface in the central tubing of $h_{tub} = (\rho_b - \rho_h)\, h / \rho_b$ (or h_{tub} = 250 m when h = 1000 m; see Figure 6).

An example of such a test was described by Hugout (1988) for a 950-m deep cavern with a volume of 8000 m^3 belonging to the Etrez site (Ain, France) operated by Gaz de France: the pressure drop (when hydrocarbon was vented) was 3 MPa. The test measures the hydrocarbon outflow rate. For several days, the hydrocarbon outflow rate is quite large, as transient creep and additional dissolution play an active role (Figure 14). After a couple of weeks, the hydrocarbon outflow rate becomes more or less constant (and much larger than the outflow rate should be in a brine outflow test —clear proof of the non-linear effect of cavity pressure on cavern closure rate.)

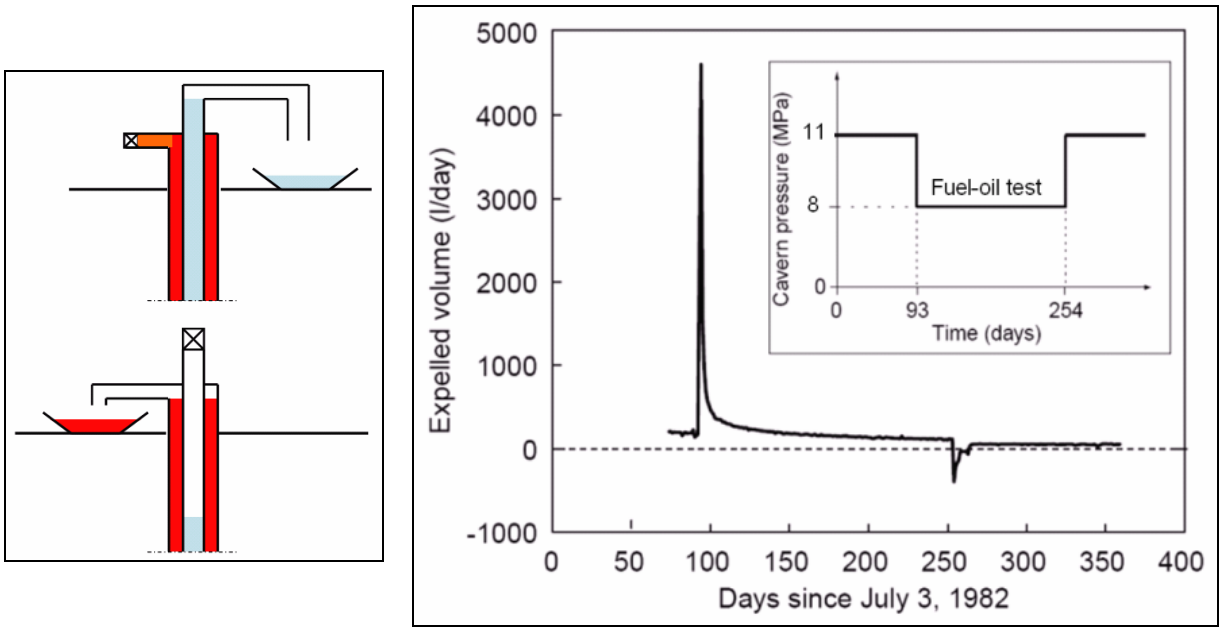

Figure 14 – Hydrocarbon Outflow Test: From day 93 to day 254, the cavern pressure was lowered below halmostatic, resulting in large transient hydrocarbon flow followed by a more-or-less steady-state hydrocarbon flow. The hydrocarbon flow rate is larger than the brine flow rate before the pressure changed on day 93 or the brine flow rate after the initial pressure had been restored on day 254 (Hugout, 1988).

Precise interpretation of this test is not straightforward, as transient creep effects can last a long time after pressure changes.

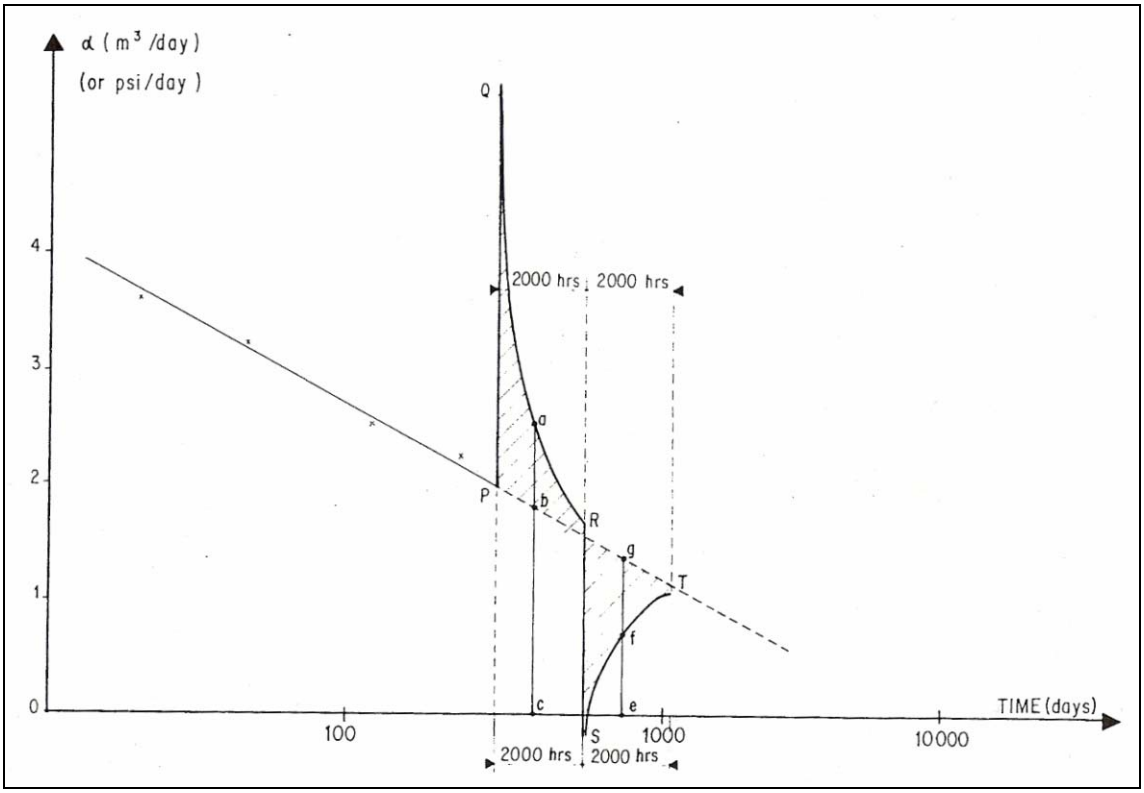

Figure 15 - Oil Outflow Test (Clerc-Renaud and Dubois, 1980).

A similar test has been described by Clerc-Renaud and Dubois (1980) for a 569 to 864-m deep cavern with a volume of 235,000 m^3 belonging to the Manosque site (South Eastern France) operated by Geostock. The cavern was filled partly with oil; oil volume was 185,000 m^3. The wellhead oil pressure was 550 psi before the test. (The wellhead brine pressure was zero.) The wellhead oil pressure was released (PQ on Figure 15), and the brine/air interface dropped in the central string. Oil outflow was measured for 2000 hours (PR on Figure 15), after which brine was injected in the central tube to increase the wellhead oil pressure by 550 psi (RS on Figure 15). Brine outflow then was measured for 2000 hours (ST on Figure 15). Note that as the cavern is partly filled with oil, separate convection cells develop both inside the brine body and inside the oil body. Oil warming is faster, as the heat capacity of oil is larger than that of brine, and heat transfer also takes place at the oil/brine interface. The oil thermal expansion coefficient also is larger than brine's. Fast convergence rates following a pressure decrease (phase PR) and "reverse" convergence following a pressure increase (phase ST) were observed .

4.2.3. Immerged Pump

A still lower pressure can be tested in a brine-filled cavern by lowering an immerged pump in the well. Röhr (1974) describes such a test performed in the Kiel 101 cavern (Figure 9). This cavern had been leached out between the depths of 1305 m and 1400 m. Due to the high amount of insolubles, less than 60% of the total 68,000-m^3 volume was available for storage. Natural gas was to be stored in this cavern, and it was decided to lower the brine pressure to investigate the cavern-creep closure rate as a function of cavern pressure. An immerged pump was set slightly above the casing shoe. "Starting about 1 November 1967, the pressure at the roof of the cavity was lowered from [15.6 MPa] to practically zero by pumping the brine out of the access well" (Baar, 1977, p.147). Figure 16, presented by Baar (1977), shows the internal pressure at the roof of the cavern dropping from 13.1 MPa to 0.65 MPa in 5 days (at which stage the roof broke), then building up. (When pumping stops, large cavern-convergence rates lead to a rapid rise in brine level in the well and result in cavern pressure building up to 8 MPa after a 35-day period.

Cavern compressibility plays an important role in this process. Pressure build-up progressively results in slower convergence rates, as observed on Figure 16).

Buffet (1998) describes the case of an immerged pump being lowered in a shallow cavern to provoke deliberate collapse of a cavern whose long-term stability could not be guaranteed. A somewhat similar case history was described by Jeanneau (2005).

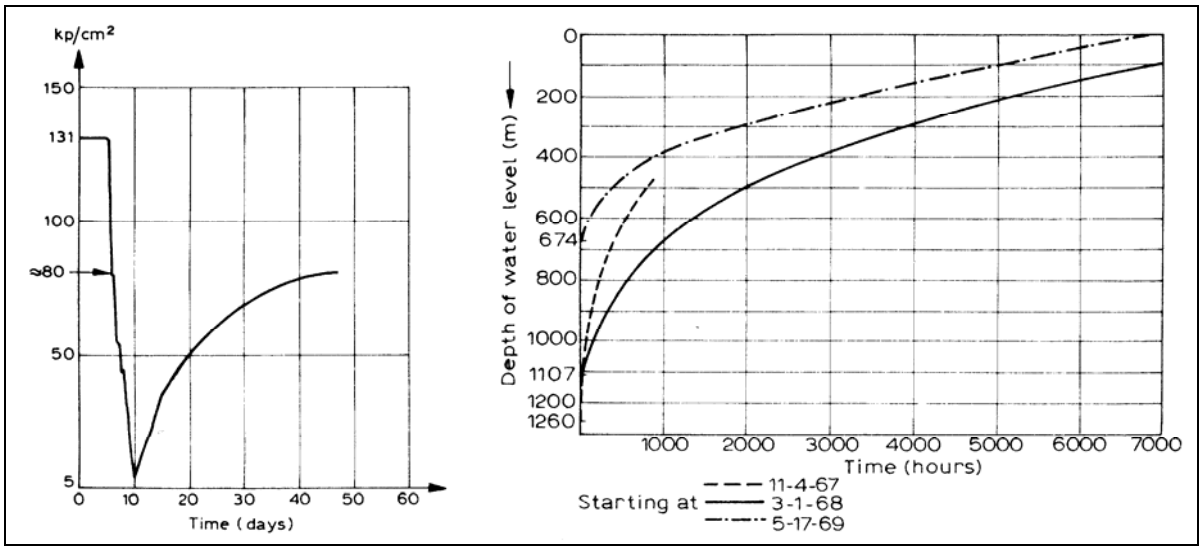

Figure 16 — Internal pressure at the roof of the Kiel 101 cavern during dewatering of the access well in November 1967 and the brine-level rise in the well after the brine level was lowered at the indicated times (after Baar, 1977); original sources are Dreyer (1972) and Röhr (1974). The initial brine level rise is rapid, but leads to slower convergence rates.

4.2.3. Other Tests

Denzau and Rudolph (1997) describe an imaginative method whose objective was to assess the effect of pressure cycles on gas-cavern convergence. The test was performed on a 380,000-m^3 cavern after 6% of the brine volume had been displaced by gas. The volume-depth function in the cavern roof (where the brine/gas interface was to be located) was precisely established before the test through sonar surveys. During the test, the evolution of the interface location was measured through γ-γ logs and through a pressure-temperature gauge lowered down the well. Four pressure cycles were applied during the 180-day long test period.

Pressure changes (between minimum and maximum pressures) were larger than 10 MPa. When the gas pressure was low, the cavern volume loss rate was faster, resulting in a faster gas/brine interface rise. Measurement of the interface displacements allows cavern convergence to be back-calculated as a function of time. It was observed (see Figure 17) that the convergence rate was most severe during the first cycle; conversely, pressure build-up during each injection phase led to a slight - increase in cavern volume — i.e., *in situ* "reverse" creep.

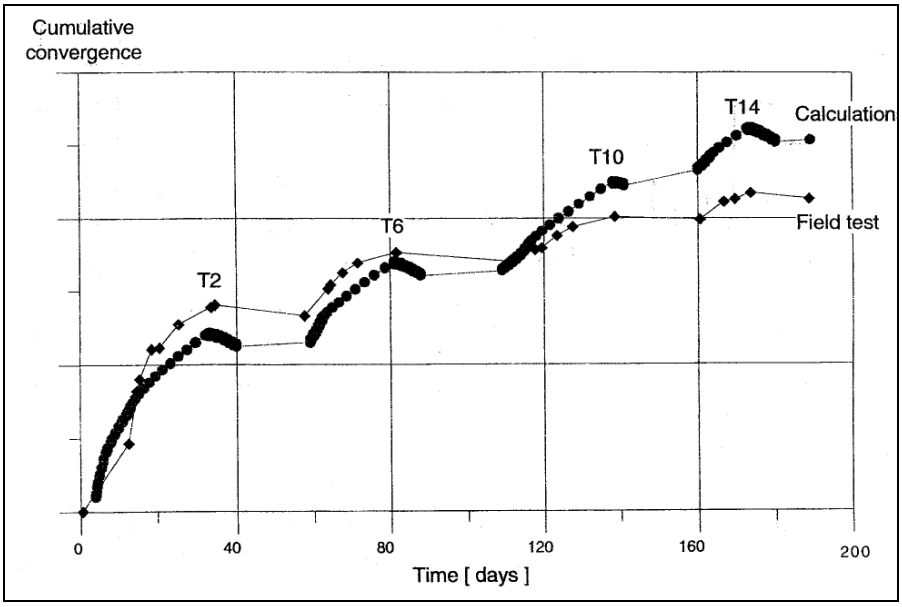

Figure 17 – During this test, four pressure cycles were applied; 6% of the cavern brine volume had been displaced by gas. Convergence was assessed through measuring the brine/gas-interface displacements (Denzau and Rodolph, 1997).

4.3. Shut-In Pressure Tests

This test probably is the most common "*in situ*" test performed in salt caverns. Interpretation is not straightforward, as brine warming (and, to a lesser extent, brine permeation or casing leaks) combine with cavern creep closure to increase cavern pressure. A few examples are described below (Figure 18 to Figure 21).

4.3.1. The Etrez 53 Test

A shut-in pressure test began on day 365 (i.e., 365 days after leaching was complete). The wellhead pressure was measured in the hydrocarbon-filled annular space (Figure 18a). Temperature evolution had been measured before the test. Most of the pressure build-up can be explained by the effect of brine thermal expansion; creep closure plays a minor role (Figure 18b).

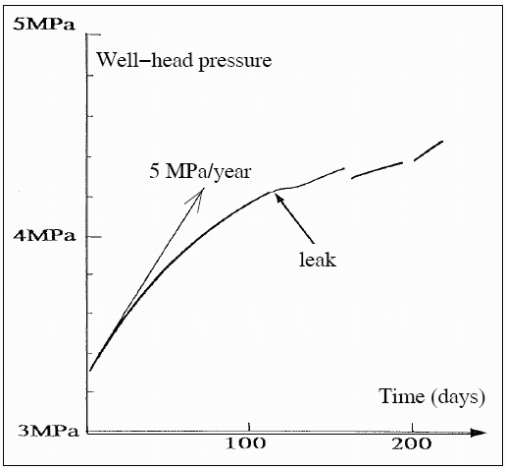

Figure 18a - Etrez 53 shut-in pressure test (after Bérest *et al.*, 2000).

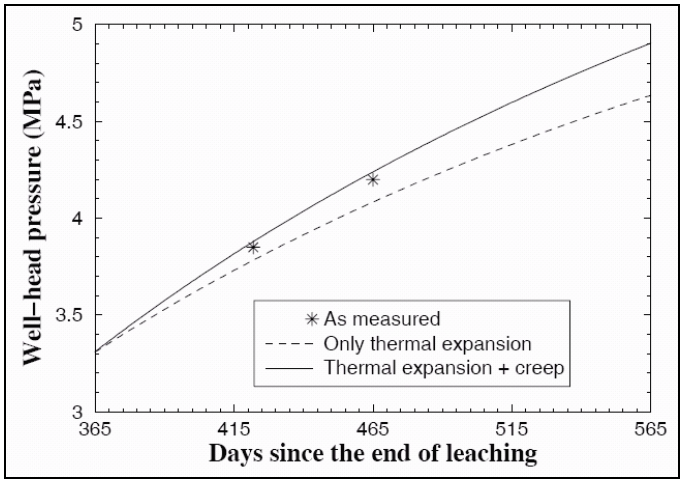

Figure 18b - Etrez 53 test interpretation: In this 950-m deep cavern, one year after the cavern was leached out, pressure build-up results mostly from brine thermal expansion (after Bérest *et al.*, 2000).

4.3.2. The Hauterives Test

The Ha6 and Ha7 caverns are connected through hydrofracturing, and the pressure evolutions in the two caverns during the shut-in tests are almost perfectly parallel (Figure 19). The (computed) effects of brine thermal expansion overestimate the as-observed pressure increase. In this case, it was suspected that small brine leaks took place through the casing and/or the wellhead. (Such a leak was observed and repaired on day 60.)

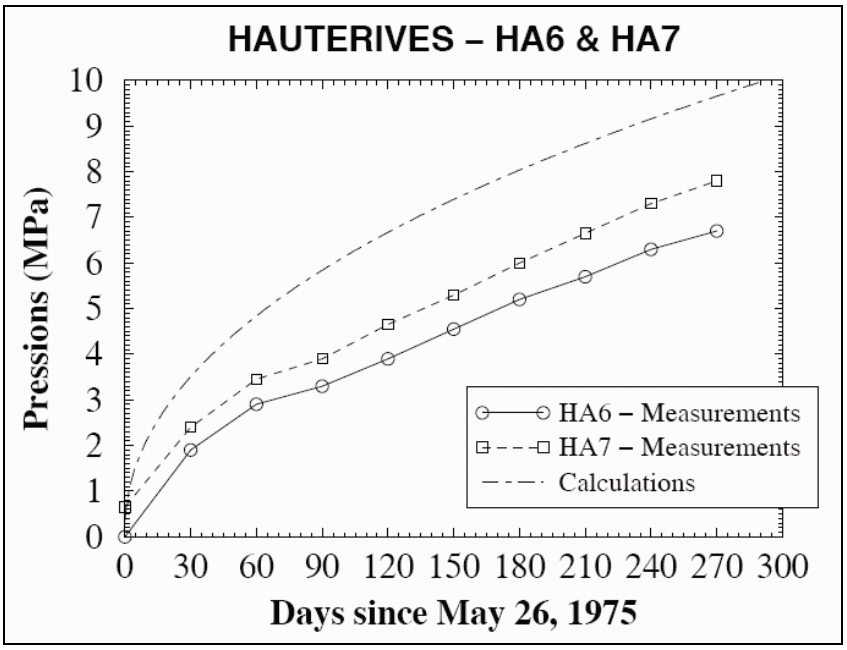

Figure 19 – Hauterives shut-in pressure test (after Bérest et al., 2000).

4.3.3. The Vauvert Test

Shut-in pressure tests were performed on the Pa1, Pa2, Pa3 and Pa6 caverns (Figures 20 and 21). In sharp contrast with the tests mentioned above in this section, the pressure build-up rate is widely underestimated when only brine thermal expansion is taken into account. In these very deep caverns (1800 to 2000 m), creep closure is extremely fast at the beginning of the shut-in pressure test, when cavern pressure is low. The creep rate becomes slower when cavern pressure increases; fracturing is reached when the cavern brine pressure is close to the geostatic pressure.

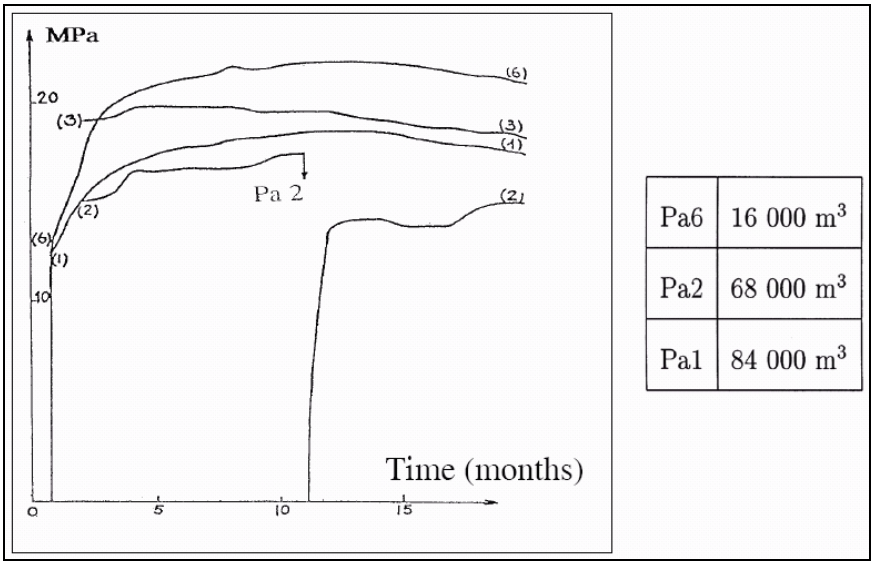

Figure 20 – Pa1, Pa2, Pa3, Pa6 shut-in pressure tests (after Bérest et al., 2000).

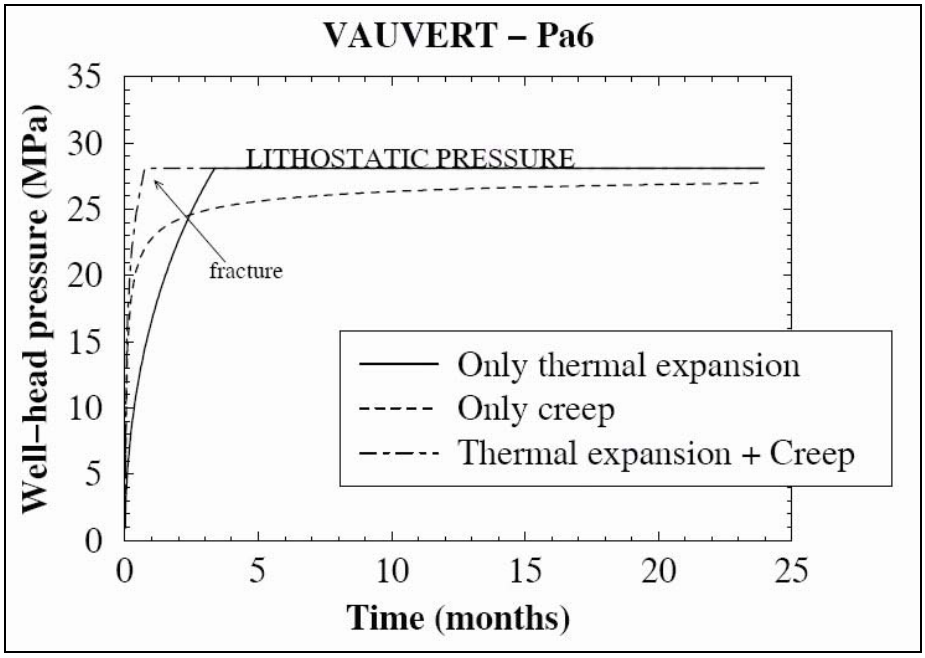

Figure 21 – Pa6 test interpretation: In this deep (1800-m to 2000-m) cavern, cavern creep closure is effective, in sharp contrast to what happens in shallower caverns (after Bérest et al., 2000).

5. *IN SITU* TESTS IN BOREHOLES

5.1. Introduction

Both shut-in-pressure tests and liquid-outflow tests can be performed on boreholes before cavern leaching starts. The main factor governing pressure evolution (or flow-rate evolution) are the same as those mentioned in tests performed on full-size caverns:

(1) warming/cooling of borehole brine;

(2) casing leaks;

(3) borehole creep closure; and

(4) micro-permeation of brine through cavern walls.

However, with an extremely small "cavern" radius, the relative significance of these factors is not the same as they are in a full-size cavern. Some of these factors (brine warming and micro-permeation) are influenced strongly by cavern size: in the case of a borehole, brine warming is negligible, and brine micro-permeation plays a prominent role.

1. Thermal equilibrium is reached rapidly in a borehole, and the thermal contraction/expansion of brine can be neglected in this context. This is in sharp contrast with full-size caverns and is an important asset of borehole tests. However, before performing a test, it is best to wait a couple of weeks after drilling has been completed , to allow the thermal disturbance generated by drilling to dissipate, after which, thermal equilibrium is reached.

2. Casing leak rates are not dependent on cavern shape or size. As the volume of a borehole (and its compressibility) is much smaller than the volume (and the compressibility) of a cavern, the drop in pressure rate due to a casing leak is much faster in a borehole than in a full-size cavern even when leak rates (in bbls/day, or l/day) are identical. However, casing leaks can be assessed accurately through a procedure similar to that suggested for a full-size cavern: fill the annular space with a hydrocarbon lighter than brine and check the pressure-difference evolution.

3. The creep closure rate is a function of such factors as cavern depth, *in situ* stresses, rock and brine temperature, and cavern shape. However, it does not depend on cavern *size* (at least, when the rock formation can be considered homogeneous.): the relative volume loss rate (say, in % per year) is the same, whatever the cavern size. This is in sharp contrast with brine permeation.

4. On one hand, steady-state micro-permeation is reached rapidly in a borehole or in a small cavern; on the other, the relative brine loss rate (in % per year) is far greater in a borehole than in a full-size cavern. *Rock formation permeability can be measured conveniently in a borehole* before leaching starts.

5.2. Shut-in Pressure Test in a Borehole

A shut-in-pressure test in a borehole is a tightness test. It allows assessment of brine leaks (through observation of pressure differences) and rock mass micro-permeability (through observation of pressure). It does not provide direct information as far as rock mechanical properties are concerned. An SMRI-sponsored test to assess rock mass permeability is described in Durup (1994).

5.3. Caliper Log

The Caliper Log method was suggested by Thoms and Gehle (1983):

> "In early 1978, exploratory boreholes were drilled to depths of 5000 feet in the North Louisiana salt domes of Vacherie and Rayburn's. The exploratory boreholes were logged

several times with 4-arm caliper 'tools' over a time period of approximately four years… A final caliper logging of both holes was performed in April, 1982." (p. 28)

Closure data for the Vacherie salt dome are provided in Figure 22. The borehole pressure during the test was halmostatic (i.e., the borehole was filled with brine and no pressure was applied at the wellhead). The average borehole diameter was slightly larger than 9 in. (a 0.9-in. closure is equivalent to a 20% cross-sectional area change). The possible error is 0.25 in. A considerable variation of hole closure with depth can be observed. This result is consistent with what is known from the non-linear behavior of rock salt, but local factors also play roles. A considerable increase in hole closure occurs at a depth of about 3400 ft, or 1000 m.

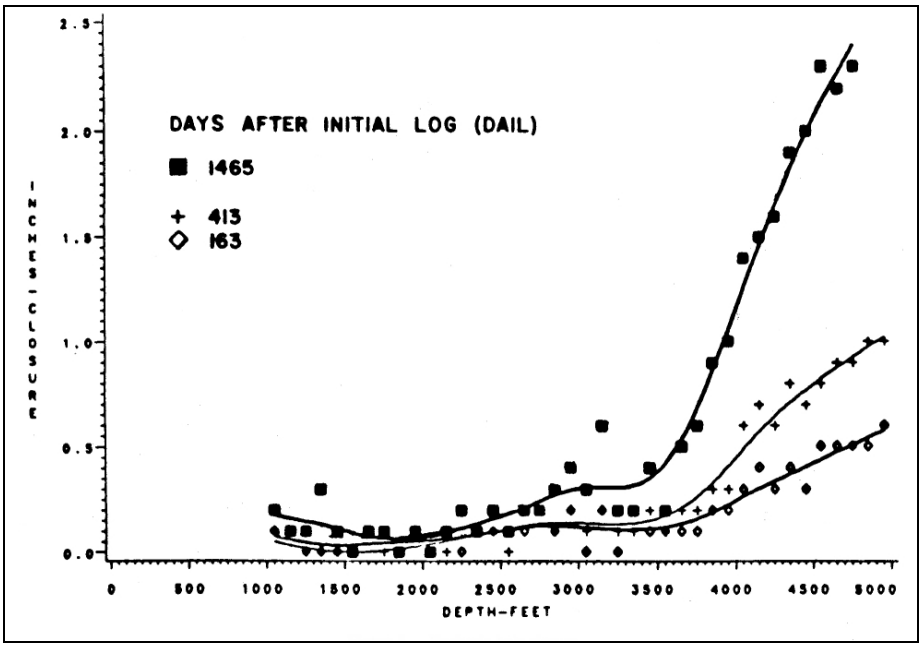

Figure 22 – Borehole diameter as a function of depth and time: The borehole closure rate is fast when the depth is greater than 3500 ft (Thoms and Gehle, 1983).

This method provides a large amount of information. (Obtaining a detailed description of borehole closure as a function of depth allows cavern implementation to be optimized.). It is costly, as a borehole must be kept idle for a significant amount of time.

5.4. Other Methods

A test using inflatable, straddle-packer test equipment is described in Nelson and Kocherhans (1984).

Estimating the stability of storage caverns (i.e., slow loss of usable volume) is especially important for natural-gas storage facilities, which experience low gas pressures (lower than halmostatic) during their lifetimes. Thoms and Gehle (1983) suggest blowing the brine from the borehole using high-pressure gas (A central string is required.) and, subsequently, lowering the gas pressure to subject the borehole to the same pressures as those planned in a storage cavern under operating conditions. Periodically the borehole (or the test interval, when a cement plug or an inflatable packer was set to isolate a specific interval) can be refilled with brine to measure loss in hole volume.

The basic principle of this test is simple, but accuracy tends to be poor when a full borehole is tested. A less severe test consists of filling the annular space with a light liquid and letting the air/brine interface drop down in the central tubing (see Section 4.2.2). However, such a test, which is probably simpler than the gas test, does not allow a large range of cavern pressures to be investigated. No description of an actual test has been found in the literature.

6. HYDROFRACTURING

6.1. Hydrofracturing in Boreholes

Hydrofracturing tests may be performed in wells, before washing out takes place, to assess *in situ* stresses. This is especially helpful when the cavern is used later to store natural gas, whose maximum operating pressure must be kept lower than the minimum *in situ* stress.

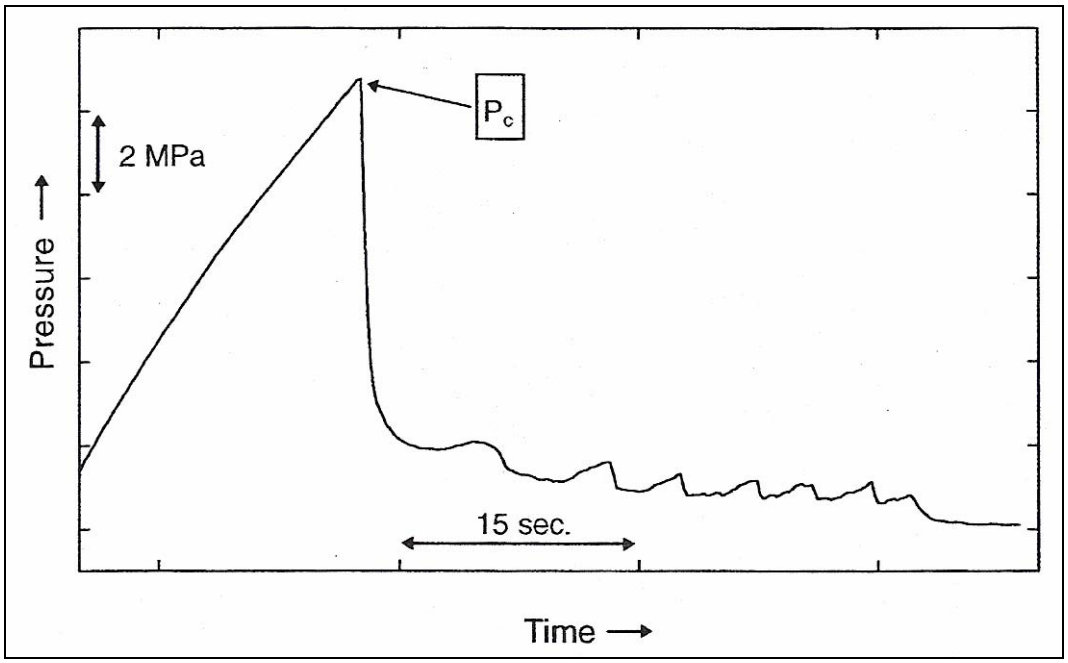

Fgure 23. Break-down pressure during an hydrofrac test (after Rummel, 1996)

Rummel et al. (1996) describe an extensive hydraulic fracturing test program, whose objective was to determine the *in situ* stress within the salt at depth at the K6 borehole of the Krummhörn gas storage facility in Germany. A total of 11 hydrofrac tests were carried out in the 8.5-in.diameter hole between 1300-m and 1800-m depth. The analysis yields a well-documented shut-in pressure profile, P_{si} (MPa) = 29.38 + 0.0194 z (m), or a shut-in pressure gradient of dP_{si}/dz = 0.0221 MPa/m for depths between 1300 m and 1720 m. Rummel et al. state that

> When we consider the characteristic hydrofrac data from all eleven tests conducted between 1305.7 m and 1721.6 m (TVD) we can observe both a systematic increase in breakdown pressure P_c with a break-down gradient P_c/TVD = 0.0255 MPa/m and in shut-in pressure P_{si} with depth with a gradient of P_{si}/TVD = 0.0221 MPa/m. The depth dependence of tensile strength as a material property is less significant with an average value of 6.3 MPa. (p.5)

They come to the conclusion that "The shut-in pressure profile is in good agreement with the vertical stress profile derived from various geophysical logs for the overburden density."

In their pioneering work, Hubbert and Willis (1957) suggested that fracturing of an impermeable, uncracked rock mass at a borehole well is reached when fluid pressure (or P_c) is such that $P_c = P_{c0} - S_h + 3S_H$, where S_h and S_H are the smaller and the larger horizontal stress, respectively, and P_{c0} is the hydraulic fracturing tensile strength, "a complex material parameter, certainly not an intrinsic material property" (Rummel et al., 1995).

For a rock-salt mass, it often is assumed that the state of stresses at depth is spherical — i.e., the main stresses are equal, $S_h = S_H = S_v$. However, anomalous stress distribution can be found (e.g., at the fringe of a salt dome).

As was pointed out first by Wawersik and Stone (1989), however, the state of stress at the vicinity of a borehole may be complex, making test interpretation more difficult. When the borehole is kept open for a long time (say, several years), brine pressure remains halmostatic, and stress redistribution slowly takes place, from the initial "elastic" distribution to the final "steady-state creep " distribution. In the process, the difference between the radial and tangential stresses is made significantly smaller than what it was when the stress distribution was "elastic". When pressure is increased rapidly in the well (as it is during a hydraulic fracturing test), the incremental stress increase is elastic, and tangential stress becomes smaller than brine pressure before brine pressure becomes geostatic, in sharp contrast with what happens during a standard hydrofracturing test in an elastic medium. Fracture pressure is significantly smaller when a test is performed after a long period of time during which cavern was kept idle.

6.2. Hydrofracturing in Salt Caverns

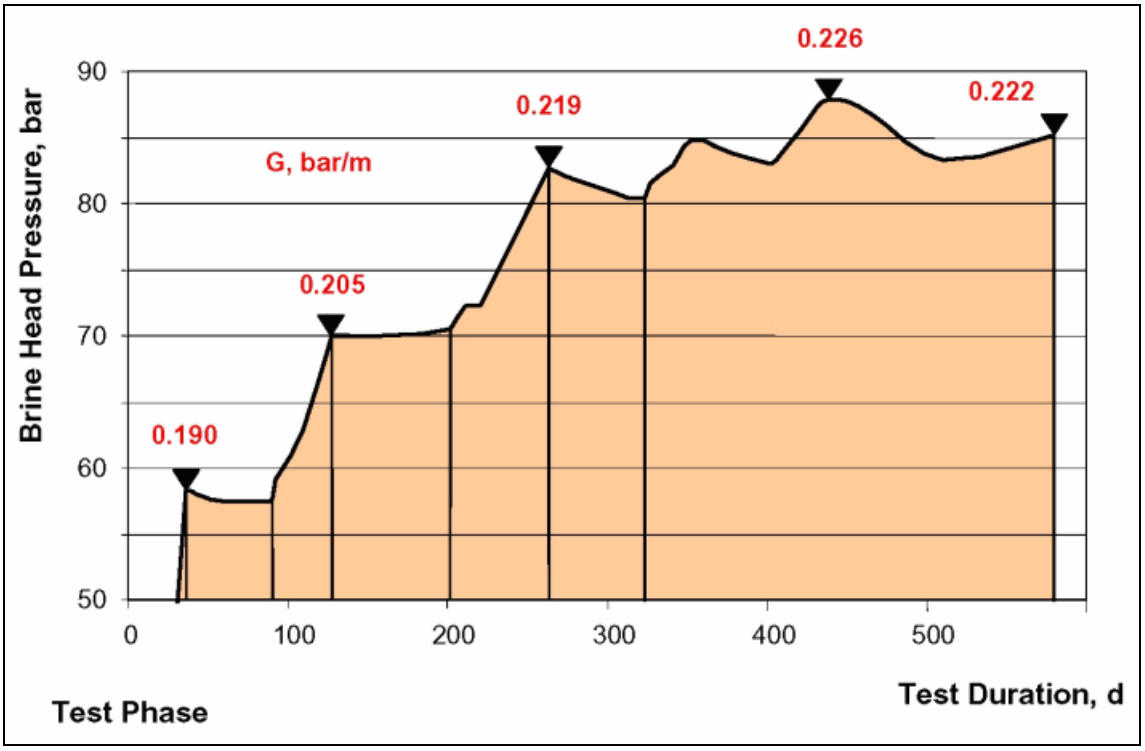

Figure 24 - Cavern pressure as a function of time during the Etzel test.

Rokhar et al. (2000) describe a test performed in 1990 in the Etzel K102 cavern, a 230,000-m^3 cavern in the cavern field located of the Etzel salt dome, 25 km southwest of Willemshaven, Germany. The cavern roof is 850 m deep. and the height of the cavern is 662 m. The objective of the test was to induce a fracture at slow pressurization rates. It was hoped that such slow rates should induce a fracture (i.e., break-down) gradient significantly higher than the fracture gradient reached during standard hydrofracturing tests. A step-by-step procedure (Figure 24) was used during the test: each pressure build-up phase was followed by an observation period lasting several weeks. The two first gradient steps were 0.019 MPa/m and 0.0205 MPa/m. A slight loss of pressure was observed following the first step, and no loss of pressure was observed following the second step. During the third step, the ratio of injected volume rate versus pressure build-up rate began to increase, clear proof of the onset of a fracture (or of increased, or "secondary", salt permeability). A gradient of 0.0219 MPa/m was reached after 7 weeks; when injection stopped, the pressure began to drop; after a two-month observation period, extrapolation to a final pressure level of 0.0217 MPa/m appeared plausible. It must be noted that the lithostatic pressure

gradient derived from borehole investigations was 0.0241 MPa/m — i.e., far larger than the gradient reached during the third step. (In hindsight, this early estimate was considered to be too high, and additional investigations have proven that the pressure gradient ranges between 0.0204 MPa/m and 0.0211 MPa/m. Re-distribution of stress in the rock mass, as explained above, also may have been influential in the early onset of a fracture (or of increased salt permeability), as the cavern had been kept idle for a long period of time before the test.

7. SUBSIDENCE

Subsidence measurement is beyond the scope of a paper dedicated to *in situ* mechanical testing. However, an SMRI technical class (2000) was dedicated to subsidence, and additional references can be found in Menzel and Schreiner (1983), Ratigan (1991), Durup (1991), Van Sambeek (1993), Quintanilha de Menezes and Nguyen (1996) and Nguyen *et al.* (1993), Bekendam and Paar (2002), Breunese *et al.* (2003). A mechanical test involving both cavern volume-loss measurement and subsequent subsidence is described in Fokker (1995).

ACKNOWLEDGEMENTS

Special Thanks to Gérard Durup and Kathy Sikora

REFERENCES

Baar C.A. (1977) Applied salt-rock mechanics, 1. *In Dlpments in Geot. Eng*. 16-A, 143–147. Elsevier Science, Amsterdam.

Bekendam R.F, Paar W.A. (2002) Induction of Subsidence by Brine Removal. *Proc. SMRI Fall Meeting*, Bad Ischl, p.49-50

Bérest P., Bergues J. and Brouard B. (1999) Review of static and dynamic compressibility issues relating to deep underground caverns. *Int. J. Rock Mech. Min. Sci.,* 36(8), 1031–1049.

Bérest P., Brouard B. and Durup G. (2000) Shut-In Pressure Tests – Case Studies. *Proc. SMRI Fall Meeting*, San Antonio, 105-126.

Bérest P., Bergues J., Brouard B., Durup J.G. and Guerber B. (2001) A salt-cavern abandonment test. *Int. J. Rock Mech. Min. Sci.* 38 (2), 343-355.

Blair R.W. (1998) Mechanical Integrity Test (MIT) Nitrogen Interface Method, *SMRI Short Course, SMRI Spring Meeting*, Houston, 7th speaker.

Boucly P. (1984) In situ experience and mathematical representation of the behavior of rock salt used in storage of gas. *Proc. 1st Conf. Mech. Beh. of Salt*, Pennsylvania, November 1981. Trans Tech Pub., Clausthal-Zellerfeld, Germany, 453-471.

Breunese J.N, van Eijs, R.M.H.E., de Meer S., Kroon I.C. (2003) Observation and prediction of the relation between salt creep and land subsidence in solution mining. The Barradeel case. *Proc. SMRI Fall Meeting*, Chester, p.38-59.

Brouard B. (1998) On the behavior of solution-mined caverns (in French). *Thesis Dissertation*, Ecole polytechnique, France.

Buffet A. (1998) The Collapse of Compagnie des Salins SG4 and SG5 Drillings. *Proc. SMRI Fall Meeting,* Roma*,*79-105.

Clerc-Renaud A. and Dubois D. (1980) Long-term Operation of Underground Storage in Salt. *Proc.5th Symp. on Salt*, Coogan A.H. and Hauber L. ed., the Salt Institute, Vol. II, 3-10.

Cole R. (2002) The Long Term Effects of High Pressure Natural Gas Storage on Salt Caverns. *Proc. SMRI Spring Meeting,* Banff, 75-97.

Colin P. and You Th. (1990) Salt Mechanics through 20 years experience at the Manosque Facility. *SMRI Spring Meeting*, Paris.

Denzau H. and Rudolph F. (1997) Field test for determining the convergence of a gas storage cavern under load conditions frequently changing between maximum and minimum pressure and its finite element modelling. *Proc. SMRI Spring Meeting,* Cracow, 71-84.

Dreyer W. (1972) The Science of Rock Mechanics, 1. The strength Properties of Rocks. Trans. Tech. Pub, Germany, 501 p.

Durup J.G. (1991) Relationship between subsidence and cavern convergence at Tersanne (France). *Proc. SMRI Spring Meeting,* Atlanta.

Durup J.G. (1994) Long term tests for tightness evaluations with brine and gas in salt. *Proc*. *SMRI Fall Meeting*, Hannover.

Ehgartner B.L. and Linn J.K. (1994) Mechanical behavior of sealed SPR caverns. *Proc. SMRI Spring Meeting*, Houston.

Fokker P.A. (1995) The Behavior of Salt and Salt caverns. *Thesis Dissertation,* Delft University of Technology, Pays-Bas.

Gaz de France (1987) Improvements in Solution Mining Techniques as Applied to Gas Storage Experienced by Gaz de France. Research Project n° 87-0001-S. *SMRI Fall Meeting*, Woodstock.

Hubbert M.K. and Willis D.G. (1957) Mechanics of hydraulic fracturing. *Trans. AIME 210*, 153-166.

Hugout B. (1988) Mechanical behavior of salt cavities -in situ tests- model for calculating the cavity volume evolution. *Proc. 2nd Conf. Mech. Beh. of Salt*, Hannover, September 1984. Trans Tech Pub., Clausthal-Zellerfeld, Germany, 291–310.

Jeanneau V. (2005) The Sinkhole of the cavity LR 50/51 in La Rape Area, a case history. RHODIA Company. *SMRI Fall Meeting*, Nancy, 9-24.

Menzel W. and Schreiner W. (1983) Results of Rock Mechanical Investigations for Establishing Storage Cavern in Salt Formations. *Proc. 6th Symp. on Salt,* B.C. Shreiber and H.L. Harner ed., Salt Institute, Vol. I, 501-510.

Munson D.E. and Myers R.E. (2000) Relative Evaluation of Storage Cavern Volume Measurements. Proc. SMRI Fall Meeting, San Antonio, 36-53.

Nelson R.A., Kocherhans J.G. (1984) In situ Testing of Salt in a Deep Borehole in Utah. *Proc. 1st Conf. Mech. Beh. of Salt*, Pennsylvania Sate University, Trans Tech. Pub., Clausthal-Zellerfeld, Geramny,493-510

Nelson P.E. and Van Sambeek L.L (2003) State-of-The-Art Review and New Techniques for Mechanical Integrity Tests of (Gas-Filled) Natural Gas Storage Caverns, 2001-4-SMRI, prepared for Solution Mining Research Institute.

Nguyen Minh D., Maitourman H., Braham S. and Durup J.G. (1993) A Tentative Interpretation of Long-Term Surface Subsidence Measurements over a Solution Mined Cavern Field. *Proc. 7th Symp. on Salt*, Kakihana H., Hardy H.R. Jr, Hoshi T., Toyokura eds. Elsevier, Vol. I, 441-450.

Quast P. and Schmidt M.W. (1983) Disposal of Medium- and Low-Level Radioactive Waste (MLW/LLW) in Leached Caverns. *Proc. 6th Symp. on Salt*, Schreiber B.C. and Harner H.L. eds., The Salt Institute, Vol. II, 217-234.

Quintanilha de Menezes J.E. and Nguyen Minh D. (1996) Long term subsidence, prediction above storage cavity fields in salt layers. *Proc. SMRI Fall Meeting*, Cleveland, 249-273.

Ratigan J. (1991) Ground Subsidence at Mount Belvieu, Texas (Panel Discussion - Surface Subsidence). *SMRI Spring Meeting*, Atlanta. Rokhar R.B., Hauck R., Staudtmeister K., Zander-Schiebenhöfer D. 2000. The Results of the Pressure Build-Up Test in the Brine Filled Cavern Etzel K102, *SMRI Fall Meeting*, San Antonio, 89-103.

Röhr H.U. (1974) Mechanical behavior of a gas storage cavern in evaporitic rocks. *Proc. 4th Symp. on Salt*, A.H. Coogan ed., Salt Institute, Vol. II, 93-100.

Rummel F., Benke K., Denzau H. (1996) Hydraulic Fracturing Stress Measurements in the Krummhörn Gas Storage Field, Northwestern Germany. *SMRI Spring Meeting, Houston.*

SMRI (2000) Technical Class on Sinkholes and Unusual Subsidence over Solution Mined Caverns and Salt and Potash Mines, *Proc. SMRI Fall Meeting*, San Antonio.

Thiel W.R. (1993) Precision Methods for Testing the Integrity of Solution Mined Underground Storage Caverns. *Proc. 7th Symp. on Salt*, Kakihame H., Hardy H.R. Jr, Hoshi T., Toyokura K. eds., Elsevier, Vol. I, 377-383.

Thiel W.R. and Russel J.M. (2004) Pressure Observation Testing Solution Mined Underground Storage Caverns in Kansas. *Proc. SMRI Spring Meeting*, Wichita, 186-198.

Thoms R.L., Gehle R.M. (1983) Borehole Tests to Predict Cavern Performance. *Proc. 6th Symp. on Salt*, B.C. Schreiber and H.L. Harner ed., Salt Institute, 27-33.

Van Sambeek L.L. (1993) Evaluating Cavern Tests and Surface Subsidence Using Simple Numerical Models. *Proc. 7th Symp. on Salt,* Kakihane H., Hardy H.R. Jr, Hoshi T., Toyokura K. ed., Elsevier, Vol. I, 433-439.

Van Sambeek L.L., Bérest P., Brouard B. (2005) Improvements in Mechanical Integrity Testing for Solution Mined Caverns used for Mineral Production or liquid-product storage. *Topical Report RSI-1799*, prepared for the Solution Mining Research Institute.

Wawersik W.R. and Stone C.M. (1989) A characterization of pressure records in inelastic rock demonstrated by hydraulic fracturing measurements. *Int. J. Rock Mech. Min. Sc. & Geomech. Abstr.,* Vol. 26, N°6, 1989, 613-628.

You Th., Maisons Ch. and Valette M. (1994) Experimental procedures for the closure of the brine production caverns of the "Saline de Vauvert" site. *Proc. SMRI Fall Meeting*, Hannover.

APPENDIX A — Comment on Transient Creep in Caverns

When submitted to a constant internal pressure, a cavern develops a long transient phase during which the rate of cavern volume loss slowly decreases, reaching steady-state creep after a very long period of time (several decades). An example of this is provided in Figure A1: a cylinder submitted to a 10-MPa axial stress and a spherical cavern submitted to a 10-MPa difference between overburden stress and cavern pressure (i.e., the case of an open brine-filled cavern at a depth of 1000 m) are considered. The axial strain rate (or relative volume-loss rate, respectively) is plotted against time. The same constitutive model was used: a Munson-Dawson model (see Munson, 1997) with parameter values of $E = 25000$ MPa , $\nu = 0.25$, $A = 0.64$ /year-MPa$^{3.1}$, $n = 3.1$, $m = 3.5$, $K_o = 6701$, $c = 0.0315$, $\alpha_\omega = -17.37$, and $\beta_\omega = -7.7$.

It can be observed (Figure A1) that transient creep is much longer in a cavern: the volume loss rate after 12 years is still larger than the steady-state volume loss rate by a factor of 1.5.

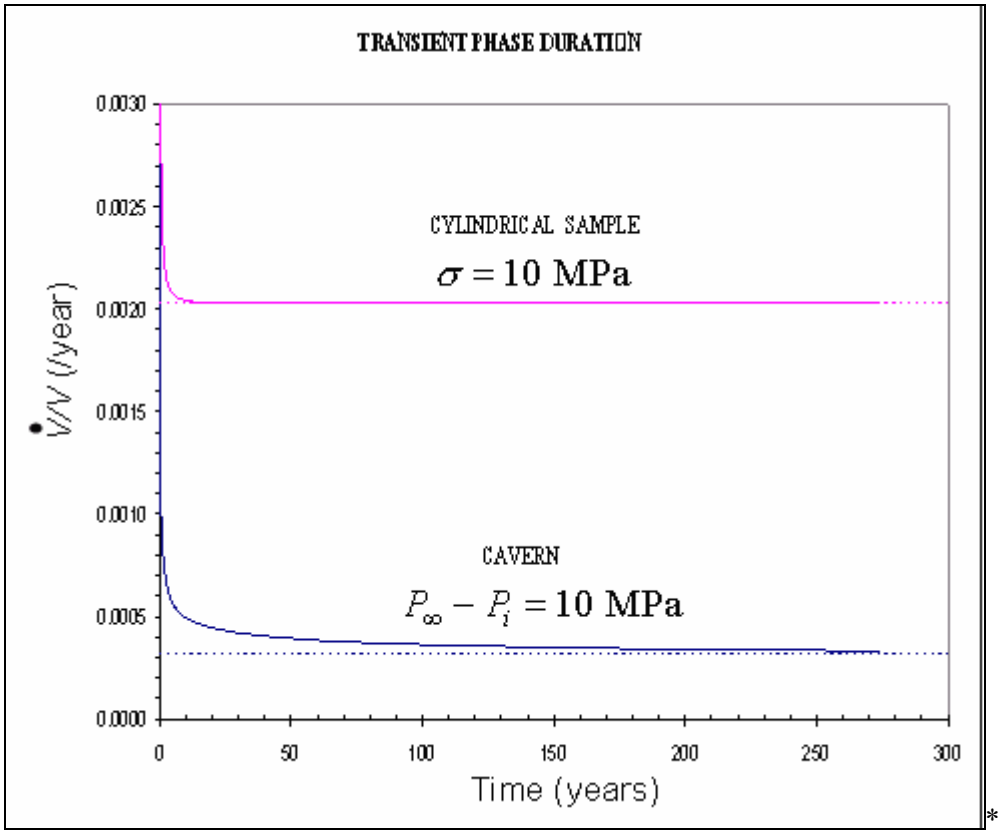

Figure A1 – Transient phase duration is much longer in an cavern than it is in a sample.

During such a transient phase, when cavern pressure is kept constant for a long period of time, stress distribution slowly evolves from the "elastic" distribution to the steady-state distribution. In particular the deviatoric stress at cavern wall slowly reduces with time.

REFERENCE

Munson D.E.(1997). Constitutive Model of Creep in Rock Salt Applied to Underground Room Closure. *Int.J.Rock Mech. Min. Sci.* Vol. 34, N°2, 233-247.